AD-A121 231 A STUDY OF THE ROLE OF GRAIN BOUNDARY CAVITATION IN THE CREEP-FATIGUE INT..(U) NORTHWESTERN UNIV EVANSTON IL DEPT OF MATERIALS SCIENCE J R WEERTMAN 20 SEP 82 1/1

UNCLASSIFIED AFOSR-TR-82-0914 AFOSR-77-3251 F/G 11/6 NL

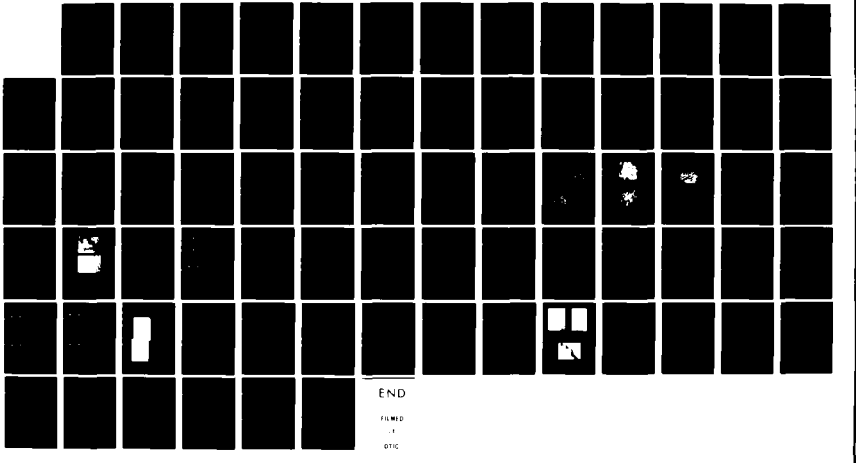

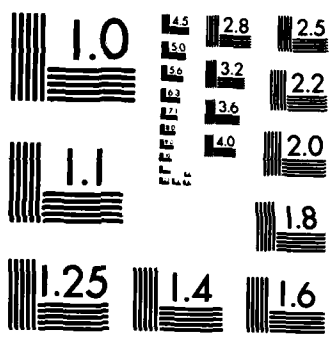

MICROCOPY RESOLUTION TEST CHART
NATIONAL BUREAU OF STANDARDS-1963-A

Unclassified

SECURITY CLASSIFICATION OF THIS PAGE *(When Data Entered)*

AD A121231

REPORT DOCUMENTATION PAGE

READ INSTRUCTIONS BEFORE COMPLETING FORM

1. REPORT NUMBER: AFOSR-TR- 82-0914	2. GOVT ACCESSION NO.: AD-A121231
3. RECIPIENT'S CATALOG NUMBER:	
4. TITLE *(and Subtitle)*: A STUDY OF THE ROLE OF GRAIN BOUNDARY CAVITATION IN THE CREEP-FATIGUE INTERACTION IN HIGH TEMPERATURE FATIGUE	5. TYPE OF REPORT & PERIOD COVERED: Final Technical Report 4/1/77 - 3/31/82
	6. PERFORMING ORG. REPORT NUMBER:
7. AUTHOR(s): Julia R. Weertman	8. CONTRACT OR GRANT NUMBER(s): AFOSR 77-3251
9. PERFORMING ORGANIZATION NAME AND ADDRESS: Northwestern University, 633 Clark Street, Evanston, IL 60201	10. PROGRAM ELEMENT, PROJECT, TASK AREA & WORK UNIT NUMBERS: 2306-A1 61102F
11. CONTROLLING OFFICE NAME AND ADDRESS: Air Force Office of Scientific Research, Bolling AFB, Building 410, Washington, D. C. 20332	12. REPORT DATE: 20 September 1982
	13. NUMBER OF PAGES: 72
14. MONITORING AGENCY NAME & ADDRESS *(if different from Controlling Office)*:	15. SECURITY CLASS. *(of this report)*: Unclassified
	15a. DECLASSIFICATION/DOWNGRADING SCHEDULE:

16. DISTRIBUTION STATEMENT *(of this Report)*

Approved for public release;
distribution unlimited.

17. DISTRIBUTION STATEMENT *(of the abstract entered in Block 20, if different from Report)*

18. SUPPLEMENTARY NOTES

19. KEY WORDS *(Continue on reverse side if necessary and identify by block number)*

20. ABSTRACT *(Continue on reverse side if necessary and identify by block number)*

1. An investigation has been carried out of the processes involved in the nucleation of grain boundary cavities in astroloy. Cavitation was produced by several methods: room temperature straining, straining and annealing, high temperature creep of prestrained astroloy, creep of non-prestrained material. It is concluded from the experimental evidence that the same mechanism is responsible for the initial grain boundary damage in all cases. In astroloy pulled at room temperature, damage shows up as microcracks at the interface

(CONTINUED ON REVERSE)

DD FORM 1 JAN 73 1473 EDITION OF 1 NOV 65 IS OBSOLETE

Unclassified

SECURITY CLASSIFICATION OF THIS PAGE *(When Data Entered)*

between carbide and matrix. It is isotropic. During annealing, large residual stresses in the strained material close up cracks on some boundaries, increase and round out the cracks on other boundaries so that damage now appears in the form of voids. Residual stresses have a large effect on the creep life of pre-strained astroloy. Their influence can persist over a significant fraction of the creep life. Residual stresses are found to be important even in the creep of non-prestrained astroloy. The density of voids in non-prestrained astroloy seems to be determined by total creep strain; it is independent of creep stress, at least over the range of test conditions studied. A small strain appears to be necessary for the onset of creep cavitation. All of the results noted above can be explained qualitatively on the basis of the stress fields which build up during deformation around non-deforming inclusions whose elastic constants differ from those of the matrix.

2. Observations have been made of the region around the tip of an intergranular fatigue crack propagating in astroloy. The fatiguing is carried out at elevated temperature under loading conditions such that the crack advances by the coalescence of grain boundary voids into the tip. Measurements of void spacing show that the voids nucleate continuously in the immediate vicinity of the crack: the spacing between voids decreases markedly with (a) decreasing distance from the end of the crack, and (b) increasing time of fatigue. (Voids as small as 20 nm in diameter are detected in this study). Values for the growth per cycle da/dN of the fatigue crack can be calculated from a knowledge of the spacing as a function of distance from the crack tip combined with a void growth law. Good agreement is found between calculated and measured values of da/dN. The threshold region of the da/dN curves also has been studied, both experimentally and theoretically. It is shown that the threshold in notched specimens is determined by the requirement that the displacement field at the notch root be large enough to permit the accommodation of the material between the coalescing voids.

DEPARTMENT OF MATERIALS SCIENCE AND ENGINEERING
THE TECHNOLOGICAL INSTITUTE
NORTHWESTERN UNIVERSITY
EVANSTON, ILLINOIS

Final Technical Report

A STUDY OF THE ROLE OF GRAIN BOUNDARY CAVITATION IN THE CREEP-FATIGUE INTERACTION IN HIGH TEMPERATURE FATIGUE

For the Period

1 April 1977 to 31 March 1982

Principal Investigator:

Julia R. Weertman, Professor of Materials Science and Engineering

September 1982

ABSTRACT

1. An investigation has been carried out of the processes involved in the nucleation of grain boundary cavities in astroloy. Cavitation was produced by several methods: room temperature straining, straining and annealing, high temperature creep of prestrained astroloy, creep of non-prestrained material. It is concluded from the experimental evidence that the same mechanism is responsible for the initial grain boundary damage in all cases. In astroloy pulled at room temperature, damage shows up as microcracks at the interface between carbide and matrix. It is isotropic. During annealing, large residual stresses in the strained material close up cracks on some boundaries, increase and round out the cracks on other boundaries so that damage now appears in the form of voids. Residual stresses have a large effect on the creep life of prestrained astroloy. Their influence can persist over a significant fraction of the creep life. Residual stresses are found to be important even in the creep of non-prestrained astroloy. The density of voids in non-prestrained astroloy seems to be determined by total creep strain; it is independent of creep stress, at least over the range of test conditions studied. A small strain appears to be necessary for the onset of creep cavitation. All of the results noted above can be explained qualitatively on the basis of the stress fields which build up during deformation around non-deforming inclusions whose elastic constants differ from those of the matrix.

2. Observations have been made of the region around the tip of an intergranular fatigue crack propagating in astroloy. The fatiguing is carried out at elevated temperature under loading conditions such that the crack advances by the coalescence of grain boundary voids into the tip. Measurements of void spacing show that the voids nucleate continuously in the immediate vicinity of the crack: the spacing between voids decreases markedly with (a) decreasing distance from the

end of the crack, and (b) increasing time of fatigue. (Voids as small as 20 nm in diameter are detected in this study.) Values for the growth per cycle da/dN of the fatigue crack can be calculated from a knowledge of the spacing as a function of distance from the crack tip combined with a void growth law. Good agreement is found between calculated and measured values of da/dN. The threshold region of the da/dN curves also has been studied, both experimentally and theoretically. It is shown that the threshold in notched specimens is determined by the requirement that the displacement field at the notch root be large enough to permit the accommodation of the material between the coalescing voids.

SUMMARY OF SIGNIFICANT FINDINGS

Studies have been carried out on (I) the mechanisms whereby grain boundary damage is produced in astroloy deformed under a variety of conditions, and (II) the process of fatigue crack propagation by the nucleation, growth and coalescence of grain boundary voids.

I. Mechanisms of Void Nucleation

1. Straining astroloy at room temperature results in grain boundary damage in the form of microcracking at the interface between carbide and matrix, close to the ends of the carbide. The cracks are associated with intense localized slip. The frequency of microcracking is roughly independent of orientation of the grain boundary with respect to the axis of straining.

2. When astroloy which had been pulled at room temperature is annealed, the cracks on boundaries oriented transverse to the stress axis shrink or disappear altogether under the influence of residual stresses; on parallel boundaries the cracks grow and round out into voids. The spacing between these voids is about the same as between the microcracks before annealing. Microcracking which occurs during room temperature straining is the mechanism whereby voids are nucleated in cold worked and annealed astroloy.

3. The residual stresses which develop during room temperature deformation of astroloy can affect creep life by over an order of magnitude.

4. The same mechanism responsible for void nucleation in astroloy strained at room temperature causes nucleation in non-prestrained astroloy during high temperature creep. It appears likely that a critical strain must be exceeded before voids nucleate. During creep, damage occurs on boundaries parallel to the creep stress direction as well as on the transverse boundaries but the stress field tends to suppress the growth of the former while promoting that of the latter. Even in material which has not been previously strained, the residual stresses which build up around the grain boundary carbides during creep are significant.

5. All of the results noted above can be explained qualitatively on the basis of the stress fields which build up during deformation around non-deforming inclusions whose elastic constants differ from those of the matrix.

II. Fatigue Crack Propagation

1. Voids nucleate continuously in the vicinity of the tip of a fatigue crack which propagates by the coalescence of grain boundary voids into the crack. Spacing between the voids is strongly dependent both on distance from the crack tip and on the duration of the fatiguing.

2. Estimates of the crack growth per cycle da/dN as a function of K_{max} can be made from calculations of void growth by vacancy diffusion used together with the measured values of void spacing. Good agreement is found between these estimates and direct measurements of da/dN. On the other hand, large errors are inherent in any theory of crack propagation based on a single fixed void spacing.

3. It has been shown, both experimentally and theoretically, that the threshold for intergranular crack propagation in notched specimens is determined by the requirement that the displacement field at the notch root be large enough to permit accommodation of the material between the coalescing voids.

DESCRIPTION OF EXPERIMENTS

INTRODUCTION

This project has been devoted to an investigation of grain boundary damage in a nickel base superalloy subjected to deformation. Particular attention has been paid to the mechanism whereby grain boundary voids are nucleated. Once the process of void nucleation is clarified, great progress will have been made toward the understanding of the so-called creep-fatigue interaction (the deviation from the non-linear superposition of the effects of static and cyclic loading on materials degradation). The project has developed two major thrusts: a study of the process of grain boundary nucleation under various conditions, and an investigation of grain boundary damage in the strain field immediately in front of a propagating fatigue crack.

MECHANISM OF VOID NUCLEATION

Preliminary experiments [1]

It has been known for some time that cold working a nickel base superalloy substantially shortens its subsequent service life at high temperatures. Dyson and coworkers [2,3] have shown that small grain boundary voids are produced in a superalloy when it is deformed at room temperature and then annealed. It is this bypassing of the normal void nucleation process which shortens the elevated temperature lifetime of the cold worked material.

The first experiments [1] on void nucleation in this project were directed towards (a) locating the preferred sites for cavity formation, and (b) identifying the source of the residual stresses which, according to Dyson et al. [3], drive vacancy flow during the annealing period in such a direction as to make the voids grow on boundaries parallel to the maximum principal stress direction and shrink on transverse boundaries.

All of the experiments described in this report have been carried out on wrought astroloy. Its composition is given in Table 1. The microstructure of

this alloy can be varied considerably by changing the heat treating schedule. Figures 1 through 4 show the microstructures that were used in the studies of void nucleation [1,4-8]. The corresponding heat treatments are given in reference [1]. It can be seen that both the grain boundary morphology and the γ' particles in the matrix are affected by the heating schedule. Extraction replicas of the grain boundary carbides are shown in Figures 5 and 6. The $M_{23}C_6$ carbides in Figure 5, which are typical of the microstructures H1-H3, are large and dendritic. Grain boundary carbides which are seen in micrographs such as Figures 1-3 actually must be cuts through the interconnected fingers. The $M_{23}C_6$ carbides in astroloy given the H-4 treatment are small and globular (Figure 6).

Small specimens of astroloy were cold rolled through a 15% RA, then annealed 2 hours at 810°C. The resulting damage was viewed by means of shadowed two stage replicas taken from carefully electropolished surfaces of the specimens. Microstructural features as small as 20 nm can be detected easily by this technique. Microcracks and voids are identified by their shadow tails in the replicas. (In none of the experiments carried out in this research has a crack or void been found in undeformed material.) Examination of a large number of replicas taken from the cold rolled and annealed specimens showed that the cavities form primarily at the ends of carbides on grain boundaries oriented approximately parallel to the rolling direction (Figure 7). Since each metal-carbide interface at the end of a grain boundary carbide is a potential void site, it is expected that a correlation exists between void spacing and carbide spacing in specimens given different heat treatments but subjected to similar deformation and annealing. Figure 8 shows that such a relationship does indeed exist. The dependence of cavitation on the orientation of the grain boundary (actually grain boundary trace) with respect to the rolling direction is given by the histograms of Figure 9. The source of the residual stress which causes voids to grow during the annealing

period on boundaries parallel to the rolling or tensile direction was identified as the difference in deformability between carbide and matrix. Tensile normal residual stresses are left at the interface between elastic carbide and plastically deformed matrix close to the ends of the carbides on boundaries parallel to the tensile stress axis (Figure 10).

Microcracking in astroloy strained at room temperature [6,8]

While qualitatively at least it became clear why voids in prestrained astroloy tend to grow on certain boundaries when the temperature is sufficiently high to permit vacancy diffusion, the nature and cause of the initial damage (the actual nucleation process) was still unknown. In an effort to learn how cold working can lead to cavitation, samples of astroloy given the H-3 heat treatment (Figure 3) were pulled at room temperature at a strain rate of 10^{-4}/sec to a strain of 1.5%, 5% or 10%. Shadowed two stage replicas of lightly electropolished surfaces revealed microcracking in the form of interfacial decohesion between carbide and matrix at the ends of the grain boundary carbides in specimens strained by as little as 1.5%. A strong correlation was observed between a crack and the impingement of a heavy slip band on the carbide at the site of the crack (Figure 11). Table 2 shows that the occurrence of the cracking is reasonably independent of the orientation of the grain boundaries with respect to the strain axis. That the cracking is not just a surface phenomenon was verified by electropolishing away some 100 μm of material and reexamining the grain boundary regions. Microcracking was found to occur here with about the same frequency as on the original surface.

A model was developed to explain the formation of interfacial microcracks close to the ends of carbides, at the point of impingement of a heavy slip trace with the carbide. Large stresses can form around grain boundary particles in material subjected to deformation, even in the absence of grain boundary sliding.

Differences in the elastic constants of particles and matrix, as well as differences in their ability to undergo plastic deformation can give rise to large concentrations of stress at the particle/matrix interface.

Figure 12 shows a grain boundary particle idealized as an ellipsoid of aspect ratio (a/b) equal to 4, a value typical of the grain boundary carbides in the astroloy heat treated according to the schedule used in these experiments. The shear modulus of the matrix is μ, of the particle is μ^*. Their Poisson ratios are ν and ν^*, respectively. The equivalent inclusion method of Tanaka and Mura [9] has been used to calculate the stresses which arise in an elastic matrix just at the interface with an elastic particle, when the ensemble is pulled by a uniaxial stress to a strain ϵ^A (measured far from the inclusion). The results of the calculation are given in Fig. 13 for the cases in which the direction of the uniaxial stress is either parallel or perpendicular to the long axis of the particle. It has been assumed that $\mu^* = 2\mu$, $\nu^* = \nu = 0.3$, and that both matrix and particle are elastically isotropic. The stresses σ_N and σ_T are defined in Figure 12; τ_{max} is the maximum value of the shear stress at the interface and on the grain boundary.

It can be seen from Figure 13 that even a modest strain ϵ^A produces large shear stresses close to the ends of the particle. In these peak regions the maximum value of the shear stress (i.e., τ_{max}) occurs on planes which lie at about 45° with respect to the long axis of the particle.

Because of the assumption of elastic behavior, because only an isolated particle is considered and thus the effects of interaction between rather closely spaced particles are ignored, and because the relationship between the elastic constants of matrix and particle must be guessed at, the calculated stresses are only an approximation to the actual stresses produced during the experiments on microcracking in astrol at roo mperature. Even so, Figure 13 explains all the observations made on the estrained specimens, albeit somewhat qualitatively.

The stresses of Figure 13 are proportional to the elastic strain ε^A, so that ever increasing stresses build up in a specimen containing hard grain boundary particles as it is being pulled. While the rest of the specimen still is in the elastic regime the large shear stresses around the ends of the particles will come to exceed the yield strength. At this point a departure from elastic behavior is expected in the form of intense localized plastic strain. Dislocations piled up against the non-deformable particles can generate enough tensile stress there to exceed the interfacial cohesive strength. Thus microcracks are produced between particle and matrix close to the ends of the particles; they are associated with intense localized slip--all just as is actually observed around the grain boundary carbides in astroloy strained at room temperature. A calculation of the critical strain ε^A needed to generate an interfacial tensile stress equal to the theoretical cohesive strength shows that, under the assumptions used to calculate the stresses of Figure 13, a strain ε^A of about 0.1% is sufficient to produce decohesion under ideal conditions. Microcracking was observed in astroloy specimens pulled at room temperature to a strain of 1.5%, the smallest strain used in the room temperature experiments.

Void nucleation in strained and annealed astroloy [4,5,8]

As found experimentally (Table 2) and predicted by Figure 13, the microcracks in astroloy strained at room temperature are distributed in a reasonably isotropic manner. However when the strained specimens are heated under zero load, a considerable change is produced in the nature of the damage. The thin microcracks on boundaries transverse to the tensile axis tend to disappear while on parallel boundaries the cracks grow into rounded voids. In the case of a specimen pulled 5% at room temperature the average microcrack length, averaged over boundaries of all orientations, was 0.12 μm. The average spacing between the cracks (on boundaries which showed a significant amount of damage) was 2.52 μm (Table 2). After the specimen was annealed in vacuum at 810°C for

two hours the cracks on parallel boundaries had rounded out into voids and almost doubled in size to an average diameter of 0.22 μm. However the void spacing on these boundaries remained almost constant, dropping only from 2.18 μm to 1.94 (Tables 2,3). The decrease in measured spacing probably occurred because a number of cracks which were too small to be detected with the replica technique grew into observable voids. The equivalence between crack spacing and void spacing is strong evidence that the formation of the decohesion microcracks during the room temperature straining is the process whereby voids are nucleated in cold worked and annealed astroloy.

Quantitative data on the strong localization of strain to regions near the ends of grain boundary carbides and on the association of voids with the impingement of a strong slip band against a carbide just at the point of damage are given in Figures 14 and 15. These results are in agreement with the predictions of Figure 13, and describe behavior observed in the samples only strained at room temperature as well as in the strained and annealed material.

In order to understand the differences in the grain boundary damage wrought by annealing the strained astroloy, it is necessary to consider the stresses which remain, even after the applied load is removed, around the non-deforming carbides in a plastically strained matrix.

Figure 16 shows the residual stresses in the matrix next to the interface with an elastic ellipsoidal particle, after the matrix has been strained plastically by the amount ε_o^p (measured far from the particle). The direction of straining is either parallel or perpendicular to the long axis of the particle. In the calculations it was assumed that once the plastic straining occurred all further response of the matrix to stress was elastic and isotropic. As before, the equivalent inclusion method of the Tanaka and Mura [9] was used to find the stresses at the particle/matrix interface.

According to Figure 16, large normal residual stresses act across the interface close to the ends of the particle. In the case of astroloy prestrained at room temperature, gradients in the large tensile normal stresses acting on grain boundary particles aligned parallel to the direction of straining drive vacancies into preexisting microcracks during the heating period. (Just at the microcrack the normal stress drops to zero, but the tensile stress persists elsewhere. It is the stress gradient which drives the vacancy flow toward the crack.) The cracks on these boundaries grow and round out into voids. On perpendicular boundaries the compressive residual stresses push vacancies out of the cracks, which thus tend to disappear (or at least become too small to be detected by the replica technique.)

Creep of prestrained astroloy [1,8]

The effect of cold working on subsequent creep life was examined in specimens which had been prestrained parallel or perpendicular to the creep stress axis. The results were compared with creep in non-prestrained material. (Experiments of a similar nature have been reported by Dyson, Loveday and Rodgers [3].) Four pairs of creep specimens were cut from specimens of the large prestrain type of Figure 17. The large specimens had been pulled at room temperature to a strain of 10% at a rate of 10^{-4}/sec. The pairs were crept to failure at several stress levels in purified argon at 750°C. The results of the creep tests are given in Figure 18, where creep fracture lifetime, t_f, is plotted against the creep stress σ. It can be seen that the orientation of the prestrain axis alters the creep life by a factor of over 20. Creep specimens prestrained by 10% in a direction transverse to the stress axis, then annealed at 750°C for 72 hours before being loaded, exhibited an even further decrease in life (closed circles in Figure 18). Dyson and Henn [2] showed that the average cavity diameter in prestrained nimonic 80A, a nickel base superalloy, first increases with time of anneal under zero applied load, then becomes time independent. They

found that, at 750°C, such void growth ceases after about 65 hours. In light of Dyson and Henn's observations it seems likely that the additional decrease in lifetime of the annealed astroloy is caused by void growth during the annealing period. In order to gain some idea of the change in t_f associated with prestraining, two non-precavitated specimens were crept to failure at 450 MPa (triangles in Figure 18). One sample was cut out parallel to the direction of the "stringers" of inclusions in the astroloy bar stock, the other perpendicular to them. Little difference was found between the lifetimes of the two samples. It does not appear that an anisotropy in creep properties is introduced by the original fabrication process. The value of t_f for the non-prestrained material is greater than that of the astroloy prestrained 10% in a direction parallel to the creep stress axis, but only by a factor of about two.

The slope of the curves in Figure 18 indicates that, at least over the stress range tested, $t_f \propto \sigma^{-3.8}$. This low stress dependence argues in favor of void growth by vacancy diffusion.

The evolution of cavitation during creep has been studied in a number of prestrained specimens which were crept for a predetermined fraction of life. After they were unloaded the specimens were lightly electropolished and the exposed surfaces examined by means of shadowed two stage replicas. Figure 19 shows the relationship between the relative frequency of cavitation on a grain boundary and its apparent orientation with respect to the creep stress axis (actually the orientation of the trace of the grain boundary) for three specimens crept at 750°C under a stress of 400 MPa. One specimen was crept for 7% of life, one for 35%, and one crept to failure. All had been prestrained 10% in a direction parallel to the creep stress axis. The results of a previous section show that at the beginning of creep the damage caused by the prestraining is distributed about equally on boundaries of all orientations. After 7% of life the majority of those cavities which are detectable by the replica technique

(> ≈ 20 nm) are located on boundaries aligned roughly parallel to the stress axis. Even after more than one third of the lifetime of a specimen has passed about as many voids are found on parallel as on transverse boundaries. At failure there is the usual preponderance of cavities on transverse boundaries. Figure 20 shows that, at only 10% of life, cavitation is almost entirely confined to transverse boundaries in specimens prestrained in a direction perpendicular to the creep loading axis.

In order to investigate more closely the growth of the voids under the influence of both the applied creep stress and the residual stresses left by prestraining, the voids in the specimens of Figure 19 were grouped according to size, i.e., < 0.10 μm, 0.11-0.20 μm, 0.21-0.30 μm, 0.31-0.40 μm, $\geq$ 0.41 μm. The relative frequency with which voids appeared in each size bracket was plotted against orientation of the boundary trace with respect to the creep stress axis (Figure 21). Figure 21a shows that after 7% of life voids of all sizes are most likely to be found on boundaries approximately parallel to the prestrain axis. At 35% of life (Figure 21b) smaller voids still show a preferance for parallel boundaries but the most extensive growth is found transverse to the creep axis. At failure all but the smallest voids are located on transverse boundaries. At all stages of creep most of the cavities appeared roughly spherical. However crack-like voids were occasionally found in the early stages of creep. This observation is consistent with the idea that prestraining nucleates voids in the form of microcracks. During the annealing period residual stresses drive vacancies into (or out of) the cracks to form voids (or heal cracks).

Figures 19 through 21 illustrate the strength and persistence of the residual stresses introduced in astroloy by room temperature straining. A 90° change in the direction of prestrain can change the creep life of astroloy by a factor of about 25 (Figure 18). For about a third of the creep life, in the case of a 10% prestrain parallel to the creep axis, the effect of the residual stresses

on void growth is comparable to, or dominant over that of an applied (creep) stress of 400 MPa (Figures 19, 21). These experiments to study the effect of prestrain on creep are similar to those carried out by Dyson, Loveday and Rodgers [3] on nimonic 80A. As in the present investigation, residual stresses were found to influence creep cavitation, although to a much lesser extent.

The stress field of a prestrained material containing hard grain boundary particles must have elements of both Figures 13 and 16. Figure 16 describes (roughly) the contribution made by the prestraining. Superimposed on these residual stresses must be the stresses produced by the creep stress, σ_{ex}, which has given rise to a creep strain ε^A (Figure 13). Obviously a linear combination of the stress fields of Figures 13 and 16 represents only a very crude approximation to the actual situation, especially because of the assumption of elastic behavior on the part of both particle and matrix (once the matrix has sustained the initial deformation ε_o^p). However such a combination field should prove valuable in explaining qualitatively the influence of prestraining on the growth of the carbides during creep.

As mentioned above, it is evident that in the earlier part of the creep life of the astroloy specimens of Figures 18-21, the residual stresses associated with prestraining are a big factor in determining the growth of the cavities. At this time the creep strain is still small, so the contribution of the stresses associated with ε^A also are small. This dominance of the residual stresses is taken into account in Figure 22 by setting $\varepsilon_o^p = 10\varepsilon^A$. Two cases are examined in Figure 22, which shows the stresses to be expected in the early stages of creep on boundaries perpendicular to the creep stress. In one situation the direction of prestrain was parallel to the creep stress, in the other it was transverse. The boundaries perpendicular to the creep axis have been singled out for special attention because it is on these boundaries that failure takes place. Figure 22 shows that, in the early stages of creep, large compressive stresses act across

the ends of the particle if the prestrain had been carried out parallel to the creep axis. These compressive stresses are located in the region most likely to have suffered microcracking during the prestraining. They act to suppress or reverse growth of the cracks on the transverse boundaries and hence increase creep life. When prestrain had been perpendicular to the creep direction the large stress contribution from the original pulling speeds up void growth. Failure is greatly accelerated.

As creep proceeds the stresses associated with the prestrain are relaxed by diffusion, dislocation climb, etc. The stress situation now more closely resembles Figure 23, in which the diminishing influence of the residual stresses has been modeled by setting $\varepsilon_o^P = \varepsilon^A$. The magnitude of σ_N across the interface close to the particle ends has diminished. (Note the change in the stress scale between Figures 22 and 23.) For both the parallel and perpendicular prestrain cases the stress across the grain boundary just outside the particles is large and tensile. Figure 13a represents the limiting situation in which the relaxation of the residual stresses is complete. Tensile stresses are present across both the interface and the grain boundary. Independent of the direction of prestrain failure is likely to occur, sooner or later, on boundaries approximately transverse to the creep stress.

Creep in non-prestrained astroloy [7,8]

The final, and most important, aspect of the study of void nucleation concerns an investigation of the nucleation mechanism during creep of non-prestrained astroloy. It will be seen that the process in non-prestrained material is similar to that operating in cold worked, and cold worked and annealed, astroloy.

All of the non-prestrained astroloy specimens were crept at 750°C in a vacuum of $\approx 1.5 \times 10^{-6}$ torr. Several stresses were used. The specimens had been polished prior to being crept. At the completion of testing each specimen was electropolished again enough to reveal underlying bulk cavitation, but not

so much as to remove the heavier slip traces. Figure 24 shows a TEM micrograph of a shadowed two stage replica of crept and polished astroloy. Except that the slip lines are slightly more diffuse and a little wiggly, this micrograph is very similar in appearance to those of prestrained and prestrained and annealed astroloy. A strong tendency for the slip traces to intersect the boundary close to the ends of carbides is evident. The results given in Figures 25 show that a slip band intersects the 20% of a carbide designated as "ends" about four times as frequently as would be expected on the basis of random encounters. This localization of strain to the carbide ends, which is similar to that observed in prestrained astroloy (Figure 14), is independent of the orientation of the boundary with respect to the creep stress axis.

The micrograph of Figure 24 shows that most of the grain boundary voids (distinguishable by their white shadow tails) are sited at the end of a carbide at the point of impingement of one or two coarse slip bands. In a specimen crept to a total strain of 5.9% under a stress of 500 MPa about 70% of the cavities were found to be associated with slip bands (Figure 26). Since inevitably some of the slip steps are polished away whereas the voids extend throughout the sample, the percentages of Figure 26 must be regarded as lower limits. The strong correlation between voids and slip bands also was seen in cavities nucleated by cold working (Figure 15). The data of Figures 26 and 27 are in accord with the common observation that creep cavities are most likely to be found on boundaries which lie transverse to the creep axis.

The number of grain boundary cavities increased as creep progressed. In order to quantify this observation the average number of voids per unit length of grain boundary trace was measured on those boundaries which lay roughly perpendicular to the creep axis. The result is plotted as a function of total creep strain in Figure 28. The density of slip bands (measured on boundaries of

all orientations) also is plotted against creep strain in Figure 28. Except for the void density point at 5.3% strain, the data corresponding to strains of less than 6% came from specimens crept at 500 MPa. The rest were from specimens crept at 650 MPa. The steady state creep rates at these two stresses were 1.4×10^{-6}/sec and 3.6×10^{-6}/sec, respectively. The straight lines in Figure 28 represent the least squares best fit through the data points. It can be seen that both the void density and the slip line density increase linearly with strain. There appears to be little dependence on stress.

A most important feature of Figure 28 is the near coincidence of the two lines. This coincidence is even more striking when it is recalled that the slip band density curve is a lower limit, since some of the slip lines are lost in the electropolishing process. On the other hand the data for the void density line came from two types of replica: replicas of the lightly electropolished surfaces and replicas made after some additional 100 μm had been removed from the surface. The void densities were found to be about the same close to the surface as at a depth below the surface grains.

The data presented in Figures 24 through 26 on creep cavitation in non-prestrained astroloy all indicate that the mechanism of void nucleation is similar to that operating during room temperature straining. The micrograph of Figure 24 and the data in Figures 25 and 26 show the same tendency for strain localization at the ends of carbides and the same association between slip trace and void at a carbide/matrix interface. Figure 28 illustrates the striking correlation between void density (measured on boundaries normal to the creep axis) and slip line density (measured on boundaries of all orientation). At least over the stress range tested (500 - 650 MPa), void spacing is determined primarily by the creep strain; it appears to be largely independent of creep stress. Dyson and McLean [10] also observed a linear relationship between void density and creep strain in nimonic 80A crept at a given stress. However they

found that the slope of the void density vs strain line varied greatly with the creep stress. This dependence on stress may be only apparent, a consequence of Dyson and McLean's measuring technique [7].

In order to explore further the similarity between the processes of void nucleation during creep and during microcrack formation at low temperatures, the density of microcracks in astroloy pulled at room temperature to a 5% strain was plotted on Figure 28 (inverted triangle). This point represents crack desnity averaged over boundaries of all orientations (Table 2). The upright triangle corresponds to the void density (on parallel boundaries only) after the strained astroloy was annealed at 810°C for 2 hours (Table 3). (The void density appears to have been increased somewhat by the annealing because, as explained earlier, very small cracks grow to a detectable size under the influence of the residual stresses during the heating period.) It is evident that, for a given strain, the density of damage produced by room temperature pulling is close to that resulting from high temperature creep.

Figure 27 confirms that creep cavities are most likely to be found on boundaries normal to the stress axis. As already discussed in connection with creep cavitation in prestrained astroloy, this result is in accord with the predictions of Figure 13. On the transverse boundaries, the portion of the interface where microcracking is most likely to occur coincides with a region of tensile normal stress. The tensile stress extends to the grain boundary adjacent to the end of the carbide so the void can continue to grow. On parallel boundaries voids also should nucleate but growth into the grain boundary region is suppressed. If material which has been crept is then annealed under zero load, the residual stress field (Figure 16) should cause a further change in the size of the voids: they would shrink on normal boundaries, grow on parallel boundaries. Figure 29 shows the relative frequency of cavitation as a function of grain boundary orientation with respect to the creep axis in astroloy crept to a total strain of 5.3%

at 750°C and then annealed without load for 2 hours at 810°C. It can be seen that the distribution has become much less anisotropic. The void density on the parallel boundaries in the crept and annealed astroloy is plotted as a square in Figure 28. Again, this density is similar to the density of the creep cavities on transverse boundaries. Residual stresses are important even in the creep of non-prestrained astroloy.

A number of workers [11-13] have observed that a critical strain must be reached before creep cavitation can begin (or at least can be detected). The points in Figure 28 of void density on transverse boundaries in crept astroloy show some scatter from linear behavior. However it does appear that the straight line of void density vs creep strain extrapolates to a finite value of creep strain at zero void density. A critical strain of 0.2% is found from the line which has the least squares best fit to the data points. (Strictly speaking, this value for the critical strain corresponds to the nucleation of voids greater than about 20 nm in diameter.)

An estimate of the critical strain ε_c^A required for the onset of creep cavitation can be made from Figure 13 by using the method described in [5]. The dislocation pile ups driven by the concentrations of shear stress near the carbide ends produce large tensile normal stresses at the particle/matrix interface just at the point of intersection with the slip plane. It is assumed that τ_{max} decays in moving along the slip plane away from the interface with a relaxation distance equal to b, the semi-minor axis of the particle. It then can be shown [5] that the largest normal stress, $\bar{\sigma}_{N,max}$, evaluated one atom distance b_o from the interface, is:

$$\bar{\sigma}_{N,max}(b_o) = 2\bar{\tau}_{max}(0)\ (b/\pi b_o)^{1/2} \qquad (1)$$

where $\bar{\tau}_{max}(0)$ is the peak value of the shear stress τ_{max} at the interface, i.e., the largest value of τ_{max} in Figure 13a. The critical strain ε_c^A to nucleate voids is found by setting $\bar{\sigma}_{N,max}(b_o)$ equal to the theoretical strength of the material, taken to be approximately E/10, where E is Young's modulus of the matrix. Since $\bar{\tau}_{max}(0)$ is proportional to ε^A, the critical strain can be found readily from Figure 13 and Equation (1):

$$\varepsilon_c^A \simeq \left(\frac{1+\nu}{90}\right)\left(\frac{\pi b_o}{b}\right)^{1/2} \qquad (2)$$

If we set $b = 2.5 \times 10^{-7}$ m (a typical value for the carbides in astroloy), $b_o = 2.5 \times 10^{-10}$ m, and $\nu = 0.3$,

$$\varepsilon_c^A \simeq 0.1\%$$

It should be noted that the stress field of Figure 13, and thus the calculated value of ε_c^A, depends on the relationship between μ^* and μ. If a relationship different from $\mu^* = 2\mu$ is assumed the agreement between observed and calculated critical strains will be affected.

The continuous nature of void nucleation during creep can be explained as follows. When the creep strain reaches the critical value ε_c^A, particle decohesion commences on those boundaries which are adjacent to grains with slip planes oriented favorably with respect to the localized shear stress τ_{max} of Figure 13. As creep proceeds void nucleation can occur on boundaries with less optimum conditions for producing decohesion.

FATIGUE CRACK PROPAGATION BY LINKAGE OF GRAIN BOUNDARY VOIDS [14,15]

Background

It is well known that, under certain conditions, crack propagation in material deformed at elevated temperature occurs by the coalescence of grain boundary cavities into the crack tip [16,17]. Voids nucleate on the grain

boundary in front of the crack, grow under the influence of the stress field surrounding it, and one by one merge into the crack tip. A number of theories of intergranular crack growth by void coalescence appear in the literature (e.g., 17-21). Details of void growth differ from one theory to another, but it seems that a common feature of all of them is the assumption that the spacing between the voids is fixed at a single value. This spacing varies neither with distance from the crack tip nor with the time that deformation has proceeded. Sometimes the value of the fixed spacing is taken to be equal to the spacing between the carbides or other hard particles on the grain boundaries [17]. It does not appear that the possiblity of changes in void spacing has been seriously considered in the theories of crack growth by void coalescence, although it is obvious that the calculated value of the crack growth rate is very sensitive to the separation between the voids.

It is the goal of the present work to examine, on as fine a scale as possible, the actual conditions in the vicinity of the tip of a crack which is advancing by void coalescence. In particular, an effort was made to look for the voids which develop in front of the crack and to measure their spacing as they march into the tip. These spacing data then are combined with a theory of void growth to obtain a crack growth rate. Finally a comparison is made between the calculated and the measured rates.

Experimental details and results

The experiments were carried out on specimens of astroloy which had been heat treated according to either the H-1 or H-4 schedule (Figures 1 and 4, [1]). In order to insure that all crack growth was intergranular, even at the high cycling frequency of 6 hz used in many of the crack propagation experiments, the astroloy was precavitated. Material to be cut into samples was cold rolled through a reduction in area of 15%, then annealed in vacuum at 810°C for two hours. Fatigue specimens were cut with their long axis perpendicular to the rolling

direction (Figure 30). As described in the first part of this report, cold rolling followed by annealing produces sub-micrometer size grain boundary voids in astroloy. Most of the voids are located on boundaries approximately parallel to the rolling direction. The 15% cold rolling and annealing procedure leads to voids spaced ≈ 5 μm apart on the parallel boundaries in the case of the H-1 astroloy. The spacing of the precavitated voids in the H-4 astroloy is about 1.5 μm.

The center notched, precavitated specimens were fatigued at 6 hz, 750°C, in tension-tension constant amplitude loading (R≈0). Testing was carried out in a vacuum of 10^{-6} torr. Crack growth was measured with a long focal length telescope sighted through a window in the environmental chamber onto the crack. While the rate of crack growth in some specimens was recorded continuously until failure occurred, the fatiguing of a series of companion specimens was interrupted at varous fractions of life and the specimens examined for evidence of damage in the region of the crack tip. Shadowed two stage replicas were used to detect grain boundary voids and other microstructural features. A composite micrograph was made of the grain boundary leading out from a fatigue crack. Void spacing was measured from the composite as a function of the distance x from the crack tip.

Figures 31,32 and 33 illustrate the typical growth pattern of voids on the grain boundary in front of an advancing fatigue crack. In Figure 31, which depicts a region somewhat in advance of the crack tip, the void density has become high but the cavities still are separated one from another. The voids in Figure 32, which was taken closer to the crack tip than Figure 31, are just beginning to coalesce. It no longer is possible to measure the spacing between individual voids. At first the voids join together to form long thin cracks but these deform into rounded dimples just before merging into the crack tip (Figure 33). Note that while the spacing between individual voids is reasonably uniform, occasionally

small gaps exist where the boundary appears to be free of cavities. It probably is the presence of these gaps which prevents the voids from immediately dissolving into the crack tip when they first begin to coalesce.

The spacing λ between individual voids which has developed by the time an H-1 astroloy sample has been fatigued through 15,000 cycles is shown in Figure 34 as a function of distance x from the crack tip. The fatigue crack has grown so that, under the loading conditions used in this test, the stress intensity factor K_{max} at the peak of the stress cycle is 32.8 MPa $\sqrt{m}$. It can be seen that the spacing between individual voids drops significantly from the value of 5 μm on transverse boundaries far removed from the plastic zone around the crack to a minimum value of about 0.2 μm some 30 to 50 μm in advance of the crack tip. Closer to the crack, voids start to coalesce and it no longer is possible to determine the spacing between the originally separate voids. Figure 35 compares the void spacing found after 12,500 cycles of fatigue (K_{max} = 24.2 MPa $\sqrt{m}$) with that produced by 15,000 cycles (K_{max} = 32.8 MPa $\sqrt{m}$). Note that, in this figure, distance from the crack tip is normalized with respect to the plastic zone size, PZS. Evidently the spacing between voids depends not only upon distance from the crack tip, but also upon the duration of the fatigue. The minimum value of the spacing, λ_{min}, which is measured at the spot in the vicinity of the crack tip where the voids are about to lose their individual identiy, is plotted as a function of K_{max} for the two microstructures H-1 and H-4 (Figure 36). The crack growth rates per cycle, da/dN, measured in precavitated samples given these heat treatments are shown in Figure 37. (Here a is one half the total crack length.)

The spacing between the dimples on fracture surfaces often is taken as being identical to the spacing between individual voids. Evidently it is the large rounded voids of Figure 33 which determine the fracture topography. A

comparison of the size of the coalesced voids in Figure 33 with the individual void spacings for the same crack given in Figure 34, will show the magnitude of the error incurred when fracture dimples are identified with individual voids.

Discussion

There are two distinct regions of the fatigue crack growth curves shown in Figure 37: the threshold region where growth of the crack just becomes perceptible, and the portion at higher values of K_{max} beyond the knee of the curve. These two sections now will be discussed in some detail.

Threshold. In order for voids near the crack tip to coalesce so that the crack can advance, somehow the material between the voids must be accommodated [17,22]. The displacement field of the crack can provide this accommodation if the spacing between the voids is not too great. For voids separated by a distance λ on the boundary the minimum displacement D required for coalescence is: $D = \beta\lambda$, where β is a constant [22]. If vacancy diffusion is responsible for void growth and coalescence, β is of the order one. Its exact value depends on the geometric pattern of the voids on the boundary. Min and Raj [22] have shown that, in the case of growth by plastic deformation, $\beta = 0.23 \exp[4/(\eta-1)]$, where η is the stress exponent in the power law creep equation. For astroloy, $\beta \simeq 0.33$. Since it seems likely that the final phases of void growth occur by plastic deformation, this value of 0.33 has been used in the present calculations.

Assume now that a precavitated, prenotched specimen is subjected to an alternating stress whose amplitude is small initially but which increases with time. The average precavitated spacing between the grain boundary voids is λ_o. Since the displacement at the crack tip D(0) is dependent on K, at first the displacement is insufficient to accommodate material between voids, even at the peak of a stress cycle when $K = K_{max}$. Eventually, however, as the stress amplitude increases, a point is reached at which K_{max} is such that $D(0) = \beta\lambda_o$ (Figure 38a). It is to be expected that the crack now will begin to grow. The critical value

of K_{max} for which coalescence just begins to occur can be identified with the threshold value of K_{max}. It should be possible to calculate the threshold value of K_{max} from the known value of λ_o and a displacement at the notch tip taken from plasticity theory. The BCS theory [23] was used to estimate D(O) as a function of K. Calculated and measured values for the threshold K_{max} for astroloy samples given the H-1, H-4, or H-3 heat treatment are listed in Table 4. It will be seen that agreement between theory and experiment is quite good.

As K_{max} is increased, the spacing between voids decreases because of nucleation in the close vicinity of the crack tip while the displacement D(x) across the crack plane increases. For all values of x less than a critical value x_c (see Figure 38b), the displacement available for accommodation of material on the grain boundary is more than sufficient to allow the voids to coalesce. Crack growth well beyond threshold. The strong dependence of the spacing between individual voids on distance from the crack tip and on time of fatigue demonstrates that void nucleation is a continuous process. Nucleation proceeds particularly rapidly in the immediate vicinity of the crack tip. It is not practical to piece together micrographs such as were used to obtain Figures 34 and 35 over the entire region needed to extend the spacing data throughout the plastic zone (several hundred micrometers). However, as a rough approximation, it can be assumed that λ varies linearly between λ_{min}, the spacing at the point in advance of the tip where voids just begin to coalesce, to λ_o at the end of the plastic zone (Figure 39a). The number of voids per unit area of grain boundary, n, is given approximately by $n = 1/\lambda^2$. As can be seen from Figure 39b, the vast majority of the voids are nucleated close to the crack tip. An average distance relative to the crack tip, <d>, traveled by a void from the time it is nucleated until it has grown sufficiently large to coalesce with its neighbors can be estimated once the void density n is known as a function of distance from the crack tip.

$$\langle d \rangle \simeq \frac{n_o \left(x_{PZS} - x_f \right)^2 - \int_{x_f}^{x_{PZS}} \frac{dn}{dx} (x - x_f)^2 \, dx}{\int_{x_f}^{x_{PZS}} n \, dx} \qquad (3)$$

where n_o is the number of voids per unit grain boundary area outside the plastic zone (assumed to be equal to the precavitated value $1/\lambda_o^2$), x_f is the distance from the crack tip at which voids start coalescing into cracks, n_f is void density at x_f, and x_{PZS} is the plastic zone size. In Equation (3) it is assumed that the contribution to <d> of the prestrain voids beyond the plastic zone is negligible. Consequently it is likely that Equation (3) underestimates <d> somewhat, particularly at small values of K_{max} where λ_{min} is closer in value to λ_o.

In order to calculate the time t_c required for an "average" void to grow from its size at nucleation to a radius which produces coalescence with its neighbors, a void growth law must be used. The following calculations are based on an equation derived by Speight and Beere [24].

$$\frac{dv}{dt} = 4\pi r^2 \frac{dr}{dt} \simeq \frac{8\pi\Omega D_B \delta}{kT} \frac{\sigma}{4 \ln(\lambda/2r) - \left[1 - \left(\frac{2r}{\lambda}\right)^2\right]\left[3 - \left(\frac{2r}{\lambda}\right)^2\right]} \qquad (4)$$

where v is the void volume, r is the radius of the void (which is assumed to be spherical), Ω is the atomic volume, D_B is the grain boundary diffusion constant, δ is the effective width of the grain boundary for the purpose of diffusion, σ is the normal stress acting across the boundary, and k and T have their usual meaning. Speight and Beere assume that void growth is limited by grain boundary diffusion, not surface diffusion, and that atoms diffusing from the voids are deposited uniformly along the boundaries. In the present analysis terms have

been neglected which arise from the influence of surface tension and gas pressure on void growth.

The calculations of <d> show that the average nucleation site is well within the plastic zone during much of a stress cycle. Therefore it seems reasonable to take the yield stress σ_o as the stress which acts across the boundary. A factor f is added to take into account the fact that a fraction of the time a void is out of the plastic zone because of the cyclic nature of the applied load. Equation (4) becomes:

$$r^2 \frac{dr}{dt} = A \frac{\sigma_o f}{4 \ln (\lambda/2r) - \left[1 - \left(\frac{2r}{\lambda}\right)^2\right]\left[3 - \left(\frac{2r}{\lambda}\right)^2\right]} \qquad (5)$$

where $A = (2\Omega D_B \delta)/kT$. At time t=0 the average void is nucleated with an initial size r_o. After a time t_c has elapsed, the void has grown until it just coalesces with its neighbors. At this time its radius must equal $\lambda_{min}/2$ just as it arrives at x_f. Note that the change in the spacing λ which the average void makes with its neighbors as it proceeds towards coalescence must be taken into account. The experimentally measured values of λ were used in the integration of Equation (5). Once t_c and <d> are known, the value of the crack growth per cycle can be calculated:

$$\frac{da}{dN} = \frac{\langle d \rangle}{\nu t_c} \qquad (6)$$

where ν is the frequency of cycling of the stress.

The calculated value of da/dN is insensitive to the value chosen for r_o. However small changes in λ_{min} profoundly influence t_c, and thus da/dN. (This fact can be seen by noting that, even if the denominator on the right hand side of Equation (5) is taken to be independent of r and λ, $t_c \propto \lambda^3$.) Equation (5) contains one disposable parameter, A, since the quantity $D_B\delta$ is unknown for

astroloy. The constant A is fixed by requiring that, for one value of K_{max} (taken as 32.8 MPa $\sqrt{m}$) the measured value of λ_{min} leads to a <d> and t_c such that $da/dN)_{calc} = da/dN)_{meas}$.

For other values of K_{max}, the value of λ_{min} was determined which would lead to the calculated values of <d> and t_c needed to give a da/dN (Equation (6)) equal to the measured crack growth per cycle. The λ_{min}'s determined in this manner are compared in Figure 40 with the directly measured values of λ_{min}. When the size of the error bars in the measured values of λ_{min} (Figure 36) and the scatter in the da/dN curves are recalled, it can be seen that the agreement is reasonable, especially in the case of the H-4 astroloy. The requirement that the observed and calculated da/dN's coincide at one value of K_{max} allows a value to be calculated for the unknown quantity δD_B. If Ω is taken as 12×10^{-30} m^3, δD_B at 750°C is found to be equal to 34×10^{-24} m^3/sec for H-1 and 79×10^{-24} m^3/sec for the H-4 astroloy. In view of the large difference in grain boundary morphology between the two microstructures it is not surprising that this variation in δD_B is found.

REFERENCES

1. T. Saegusa, M. Uemura, and J. R. Weertman, Metall. Trans. 11A, 1453 (1980).
2. B. F. Dyson and D. E. Henn, J. of Microsc. 97, 165 (1973).
3. B. F. Dyson, M. S. Loveday, and M. J. Rodgers, Proc. Roy. Soc. London A349, 245 (1976).
4. M. Kikuchi and J. R. Weertman, Scripta metall. 14, 797 (1980).
5. M. Kikuchi, K. Shiozawa, and J. R. Weertman, Acta metall. 29, 1747 (1981).
6. K. Shiozawa and J. R. Weertman, Scripta metall. 15, 1241 (1981).
7. K. Shiozawa and J. R. Weertman, Scripta metall. 16, 735 (1982).
8. K. Shiozawa and J. R. Weertman, to be published.
9. K. Tanaka and T. Mura, Metall. Trans. 13A, 117 (1982).
10. B. F. Dyson and D. McLean, Met. Sci. 6, 220 (1972).
11. R. G. Fleck, D. M. R. Taplin and C. J. Beevers, Acta metall. 23, 415 (1975).
12. N. G. Needham and T. Gladman, Metal Sci. 14, 64 (1980).
13. T. Johannesson and A. Thölen, J. Inst. Metals 97, 243 (1969).
14. B. Kirkwood and J. R. Weertman, Micro and Macro Mecahnics of Crack Growth, edited by K. Sadananda, D. J. Michel and B. B. Rath, TMS-AIME, N. Y., p. 199 (1982).
15. B. Kirkwood and J. R. Weertman, Scripta metall. 16, 627 (1982).
16. D. J. Michel and H. H. Smith, Acta metall. 28, 999 (1980).
17. R. Raj and S. Baik, Met. Sci. 14, 385 (1980).
18. D. S. Wilkinson, Mater. Sci. Eng. 19, 31 (1981).
19. V. Vitek, Met. Sci. 14, 403 (1980).
20. W. D. Nix, D. K. Matlock, and R. J. Dimelfi, Acta metall. 25, 495 (1977).
21. D. A. Miller and R. Pilkington, Metall. Trans. 11A, 177 (1980).
22. B. K. Min and R. Raj, Acta metall. 26, 1007 (1978).
23. B. A. Bilby, A. H. Cottrell and K. H. Swinden, Proc. Roy. Soc. London A272, 304 (1963).
24. M. V. Speight and W. Beere, Met. Sci. 9, 190 (1975).

TABLE 1

Composition of Wrought Astroloy

Co	16.00 - 18.00	wt %
Cr	14.00 - 16.00	
Mo	4.50 - 5.50	
Al	3.85 - 4.15	
Ti	3.35 - 3.65	
C	0.03 - 0.09	
Ni	balance	
B	0.02 - 0.03	
Fe	max 0.050	
Mn	max 0.15	
Si	max 0.20	
Zr	max 0.06	
Cu	max 0.10	
S	max 0.015	
P	max 0.015	

The composition of astroloy used in the experiments described in this paper.

TABLE 2. Extent of microcracking as a function of orientation of the grain boundary with respect to the strain axis. α is the angle between the strain axis and a grain boundary trace. The astroloy sample was pulled to a plastic strain of about 5% at room temperature.

α deg.	no. boundaries with cracks / total no. boundaries observed	no. carbides with cracks / total no. carbides observed	average crack spacing μm
0°–90°	11 / 31 = 35.5 %	85 / 291 = 29.2 %	2.52
0° ± 10°	5 / 13 = 38.5 %	39 / 121 = 32.2 %	2.18
45° ± 10°	2 / 7 = 28.6 %	15 / 64 = 23.4 %	2.94
90° ± 10°	4 / 11 = 36.4 %	31 / 106 = 29.2 %	2.43

TABLE 3. Extent of cavitation as a function of orientation of the grain boundary with respect to the strain axis. α is the angle between the strain axis and the grain boundary trace. The astroloy sample of Table 2 had been annealed at 810°C for 2 hours.

α deg.	$\frac{\text{no. voids}}{\text{total no. voids observed}}$	$\frac{\text{no. voids}}{\text{total no. carbides observed}}$	average void spacing μm
0° ± 10°	55 / 78 = 70.5%	55 / 151 = 36.4 %	1.94
45° ± 10°	16 / 78 = 20.5%	16 / 93 = 17.2 %	—
90° ± 10°	7 / 78 = 9.0%	7 / 137 = 5.1 %	—

Microstructures [1]	λ_o, μm	K_{max} at threshold, MPa $\sqrt{m}$	
		measured	calculated
H-1	5.0	19.1	19.5
H-3	2.6	16.0	16.2
H-4	1.3	15.0	14.5

Table 4. Measured and Calculated Threshold Values for K_{max}.

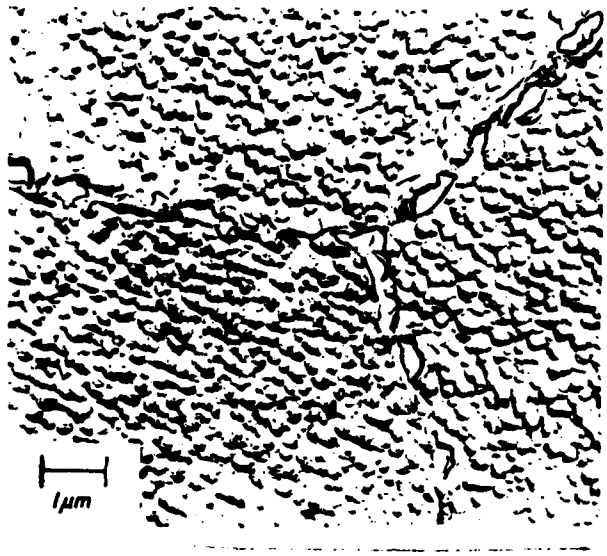

Fig. 1---Microstructure of astroloy given H-1 heat treatment.

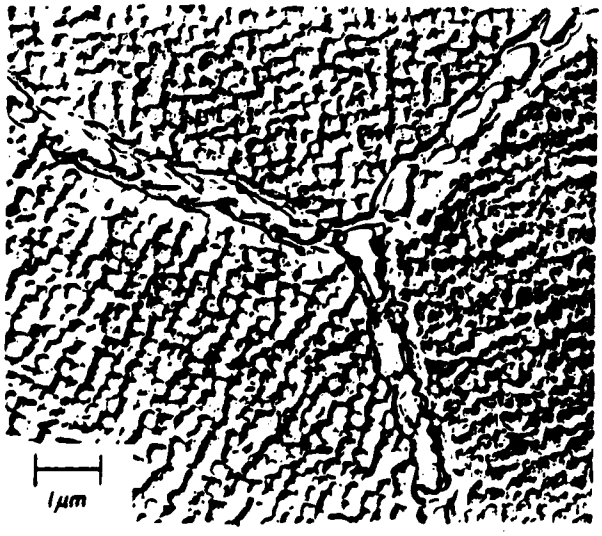

Fig. 2--Microstructure of astroloy given H-2 heat treatment.

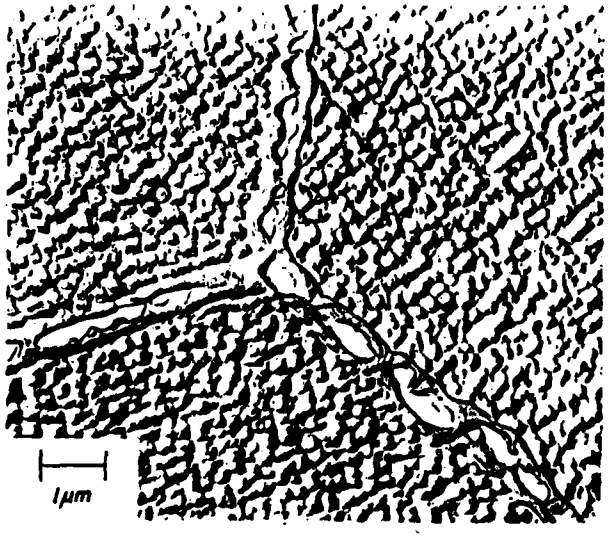

Fig. 3--Microstructure of astroloy given H-3 heat treatment.

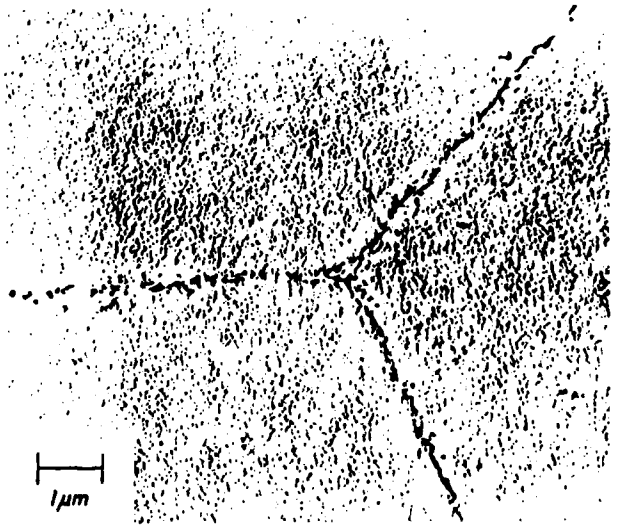

Fig. 4--Microstructure of astroloy given H-4 heat treatment.

Fig. 5--Extraction replica of grain boundary carbides from astroloy given H-3 heat treatment.

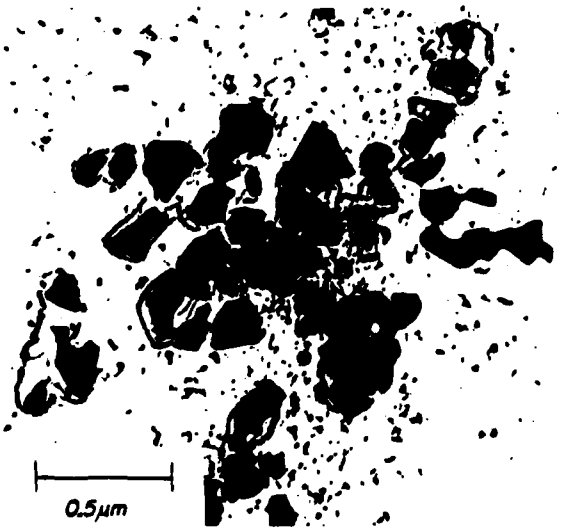

Fig. 6--Extraction replica of grain boundary carbides from astroloy given H-4 heat treatment.

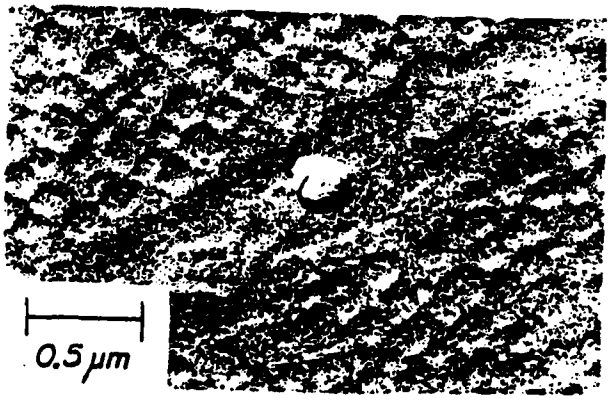

Fig. 7--Void at end of carbide in a specimen of astroloy which was cold rolled and annealed.

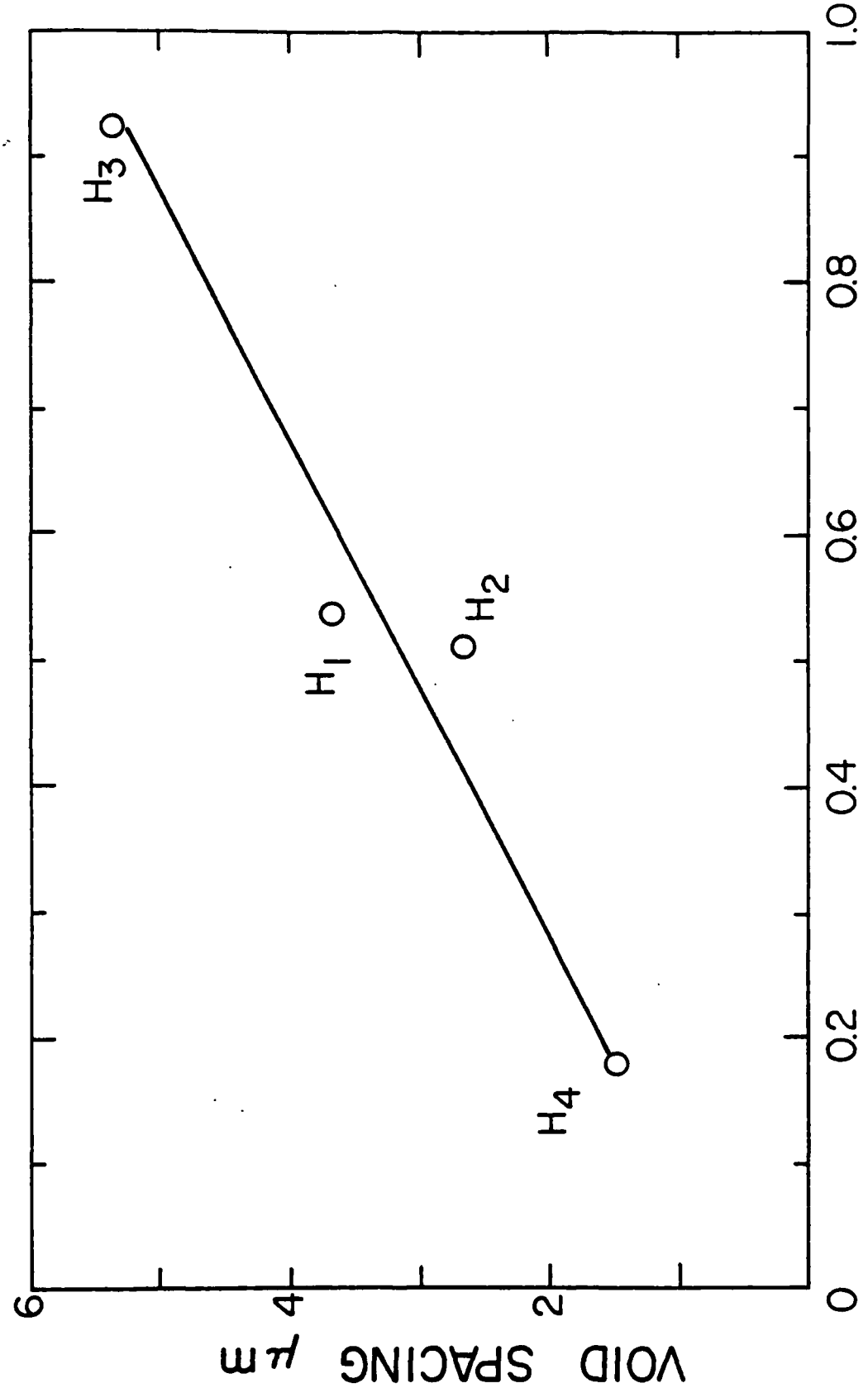

Fig. 8--Relationship between the average void spacing and the average carbide spacing in the 4 microstructures H-1, H-2, H-3, and H-4.

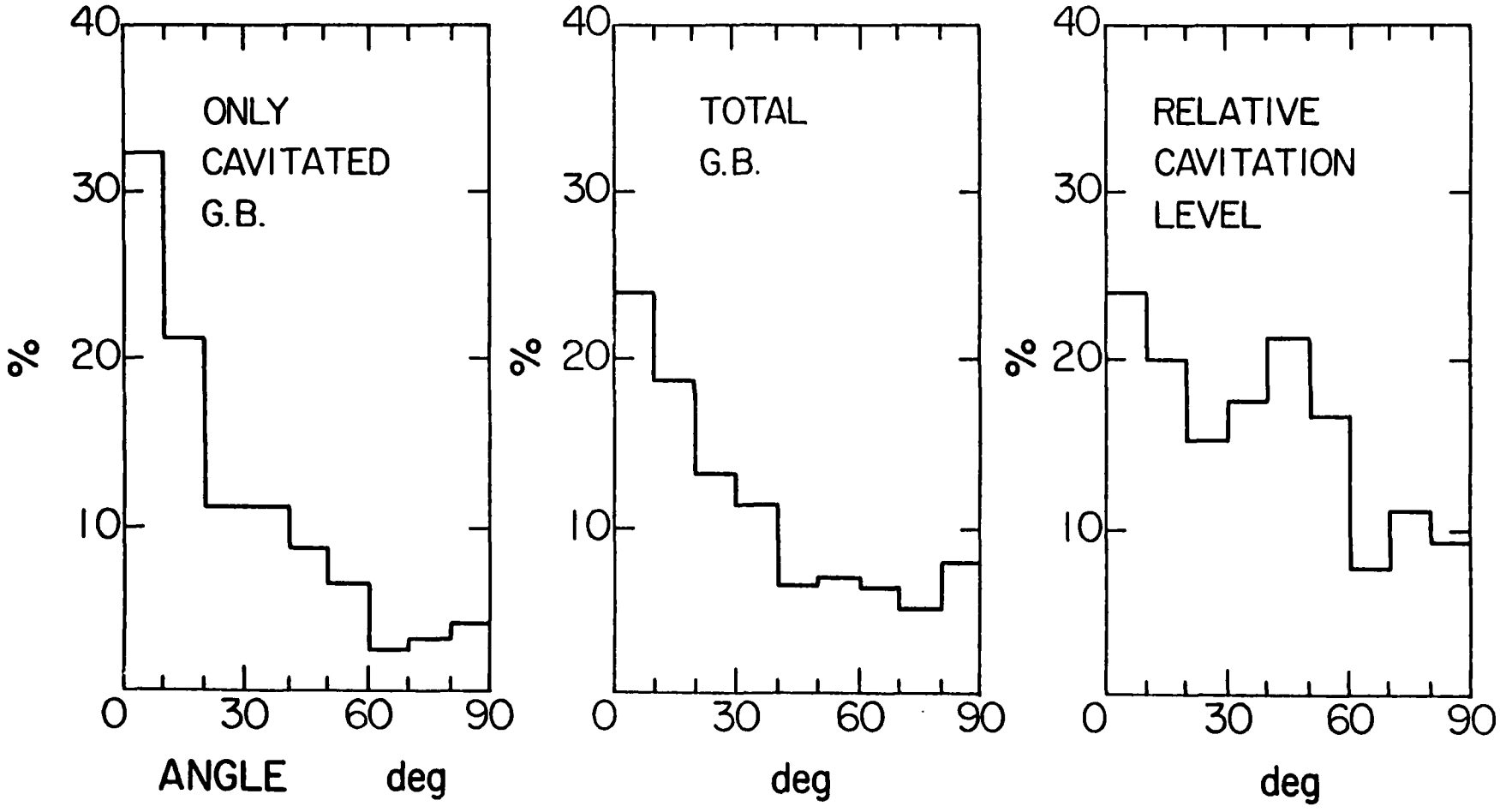

Fig. 9--Angular distribution of grain boundaries with respect to rolling direction. Astroloy, rolled 15 pct RA, annealed at 810°C for 2 hours.

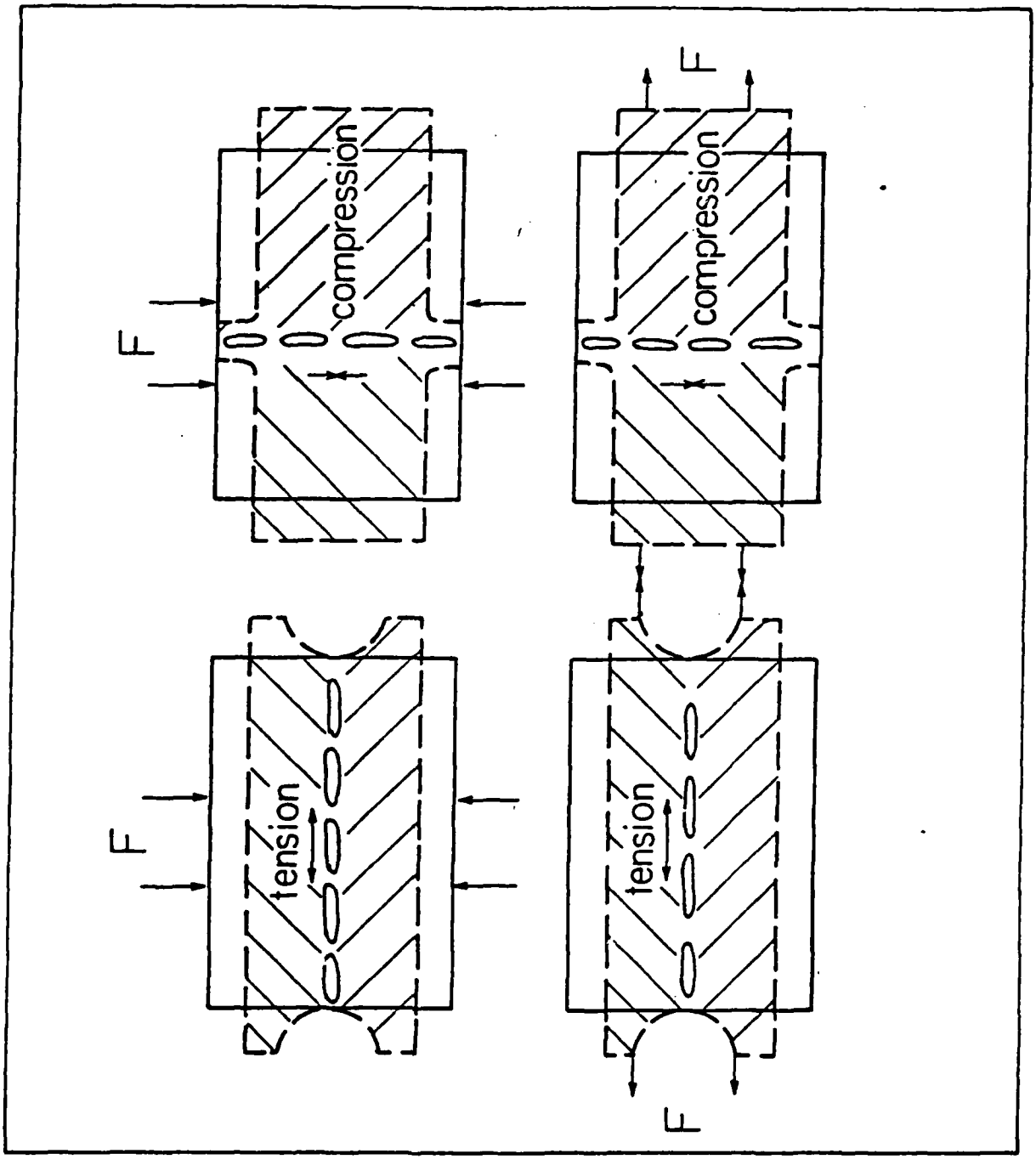

Fig. 10--Residual stresses along grain boundaries in material deformed in tension and in compression. Solid line indicates grain boundary region before deformation; dotted line the same region afterwards. The hard carbides in the grain boundary resist deformation.

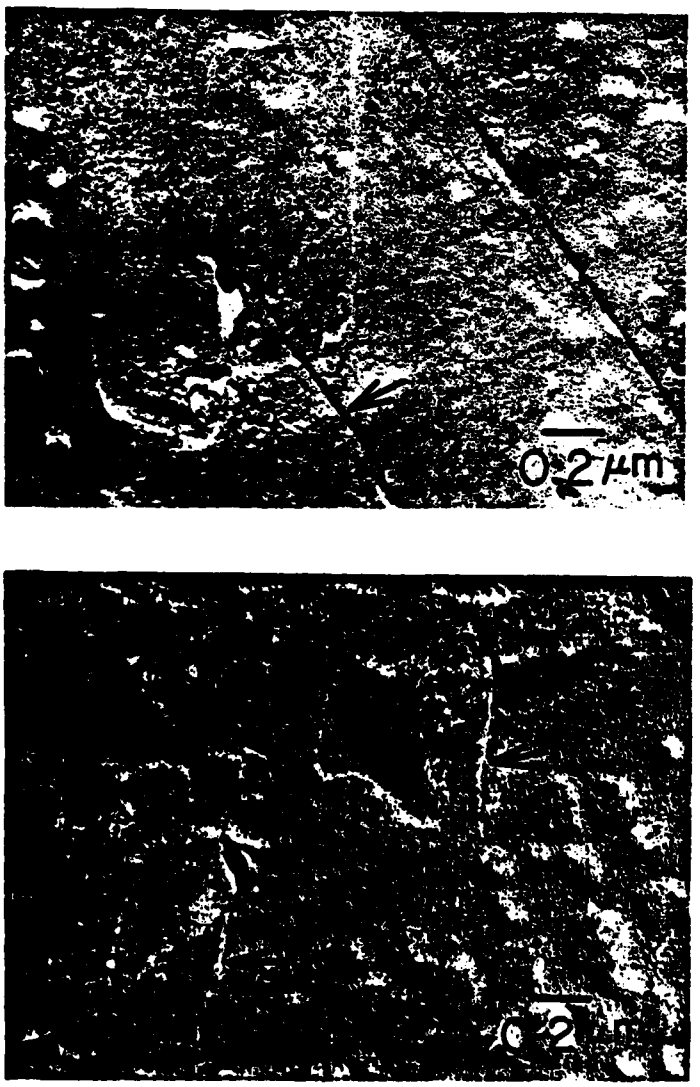

Fig. 11--Shadowed two stage replicas of a sample of astroloy which had been pulled at room temperature to a strain of about 5%. Note microcracks (confirmed by the white shadow tails) and the associated slip steps (indicated by arrows).

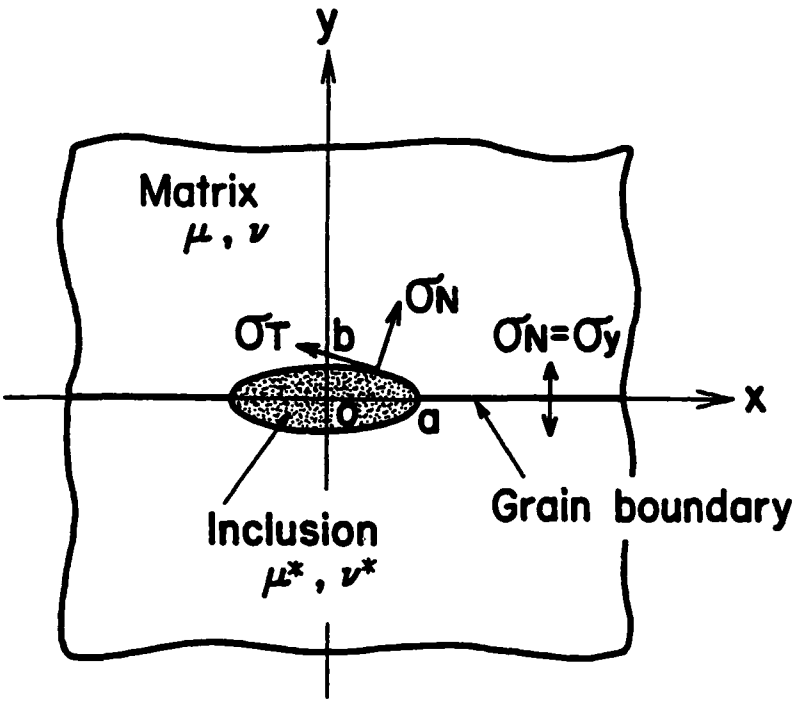

$\mu^* = 2\mu$, $\nu^* = \nu$

$b/a = 1/4$

Fig. 12--Model of an elliptical inclusion in a homogeneous matrix.

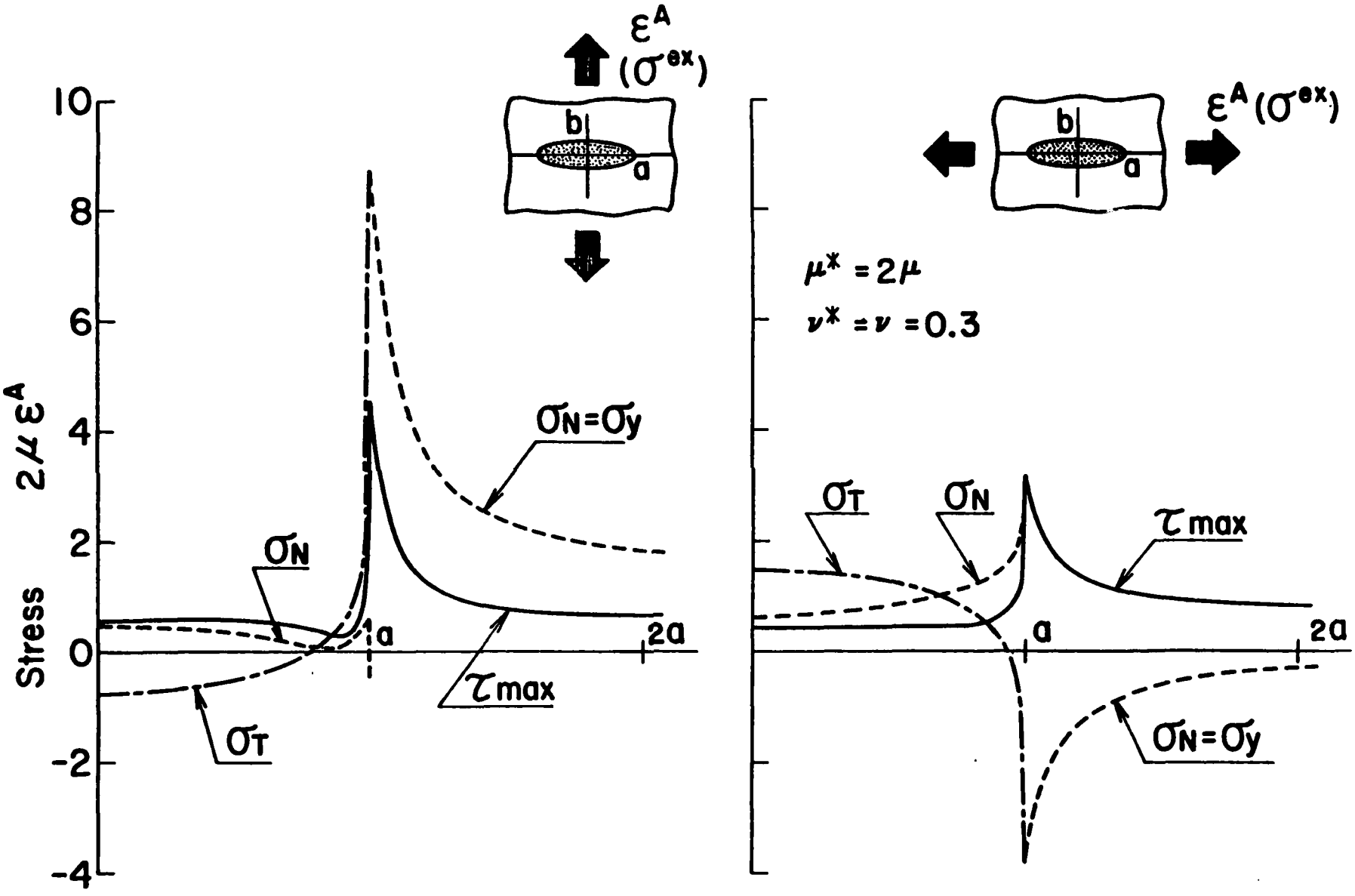

Fig. 13--Normal stress σ_N, tangential stress σ_T, and maximum shear stress τ_{max} which develop at the interface of an inclusion with the matrix when the matrix/inclusion ensemble is pulled by an external stress, σ^{ex}, to a strain ε^A (measured far from the inclusion).

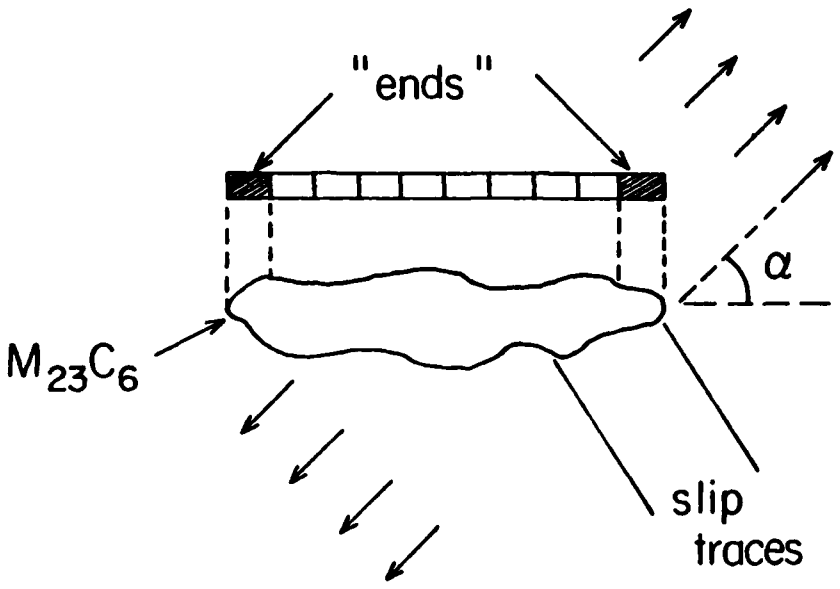

α	% Slip traces hitting a carbide end
0° ± 10°	46 / 64 = 72%
45° ± 10°	30 / 59 = 51%
90° ± 10°	29 / 47 = 62%

Fig. 14--Fraction of slip traces hitting the end of a grain boundary carbide as a function of the angle α between the stress axis and the grain boundary trace. The numerator in a fraction is the number of traces observed hitting an end; the denominator is the total number of traces observed.

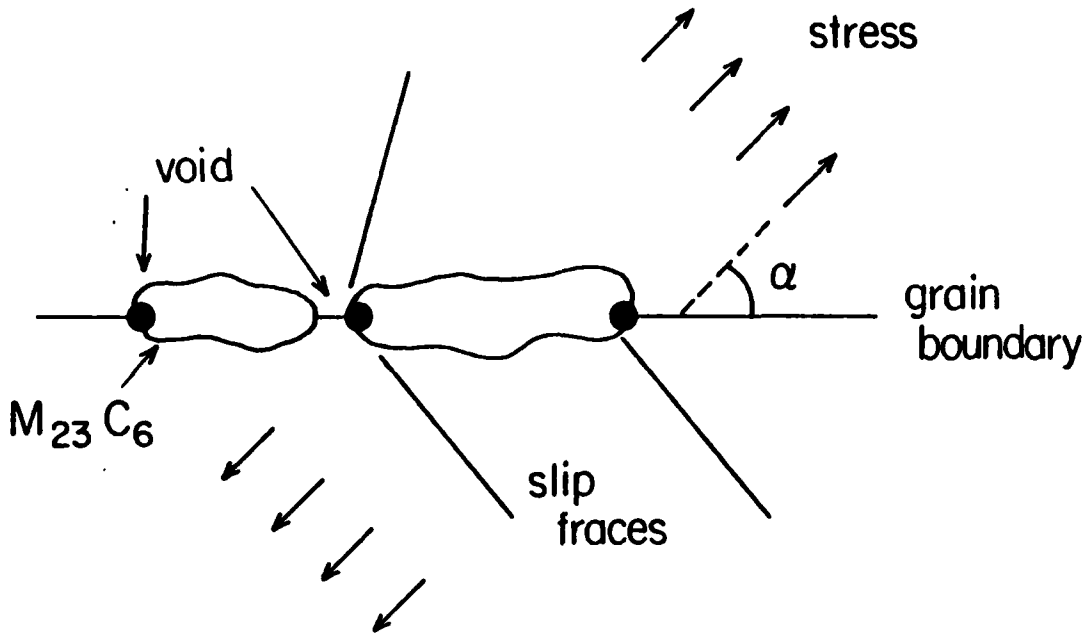

α	void with slip trace(s)	total no. voids	% voids with slip traces
0 – 90°	33	38	87
0° ± 10°	26	30	87
45° ± 10°	7	8	88
90° ± 10°	0	0	—

Fig. 15--Fraction of voids associated with one or two slip traces as a function of the angle α between the stress axis and the grain boundary trace.

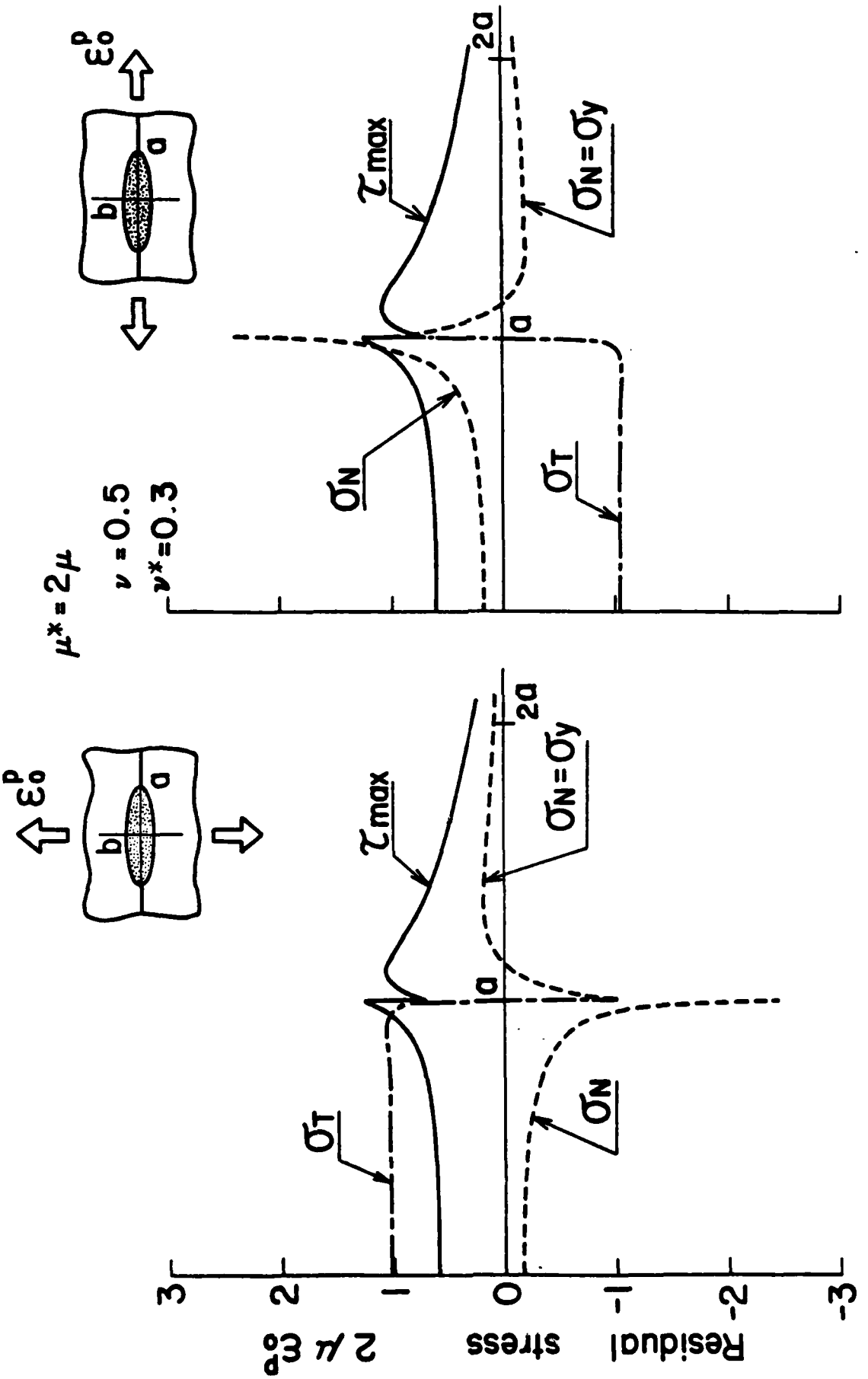

Fig. 16--Normal stress σ_N, tangential stress σ_T, and maximum shear stress τ_{max} which develop at the interface of the inclusion with the matrix after the matrix has suffered a uniform plastic deformation ε_0^p.

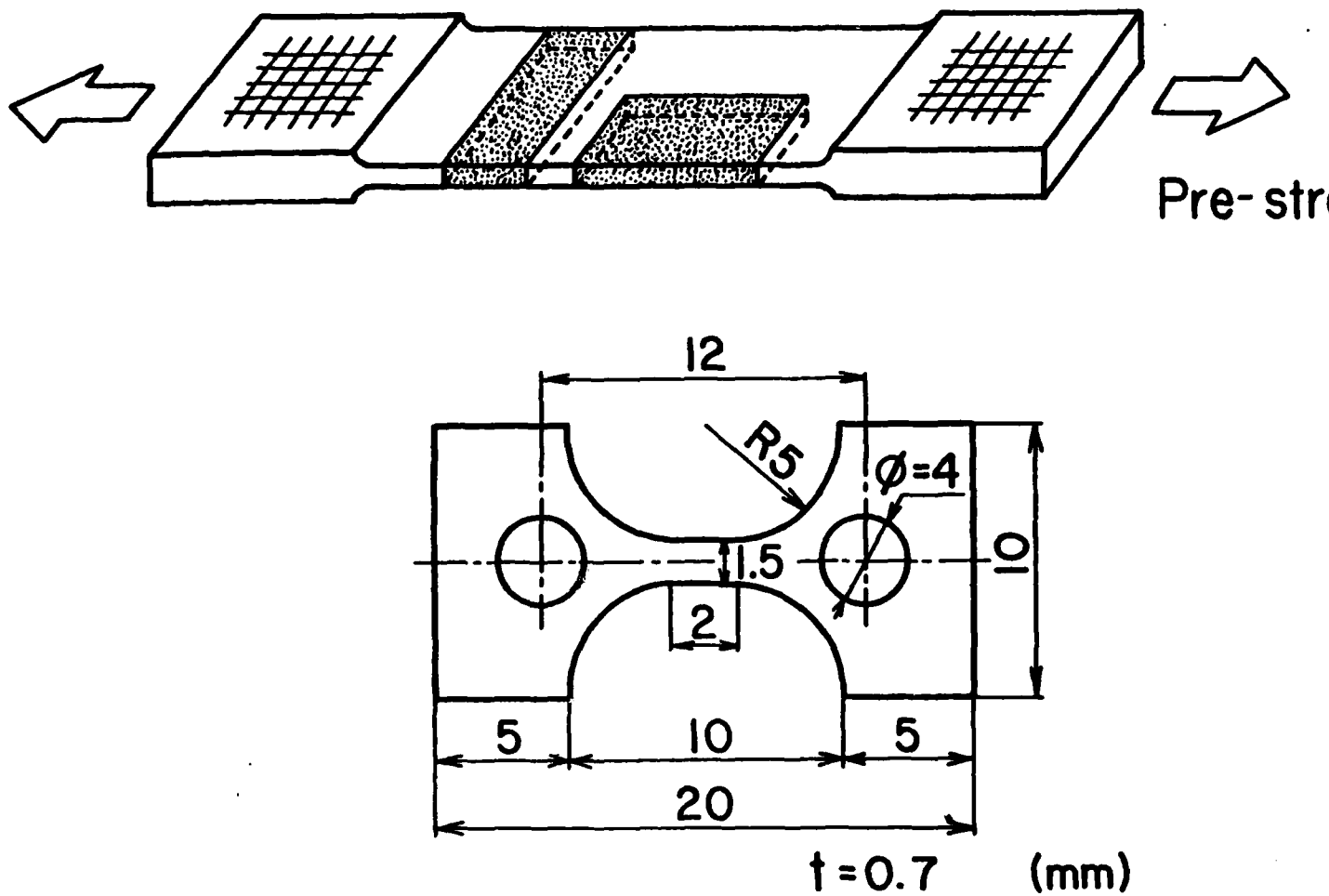

Fig. 17--Specimens used in creep experiments.

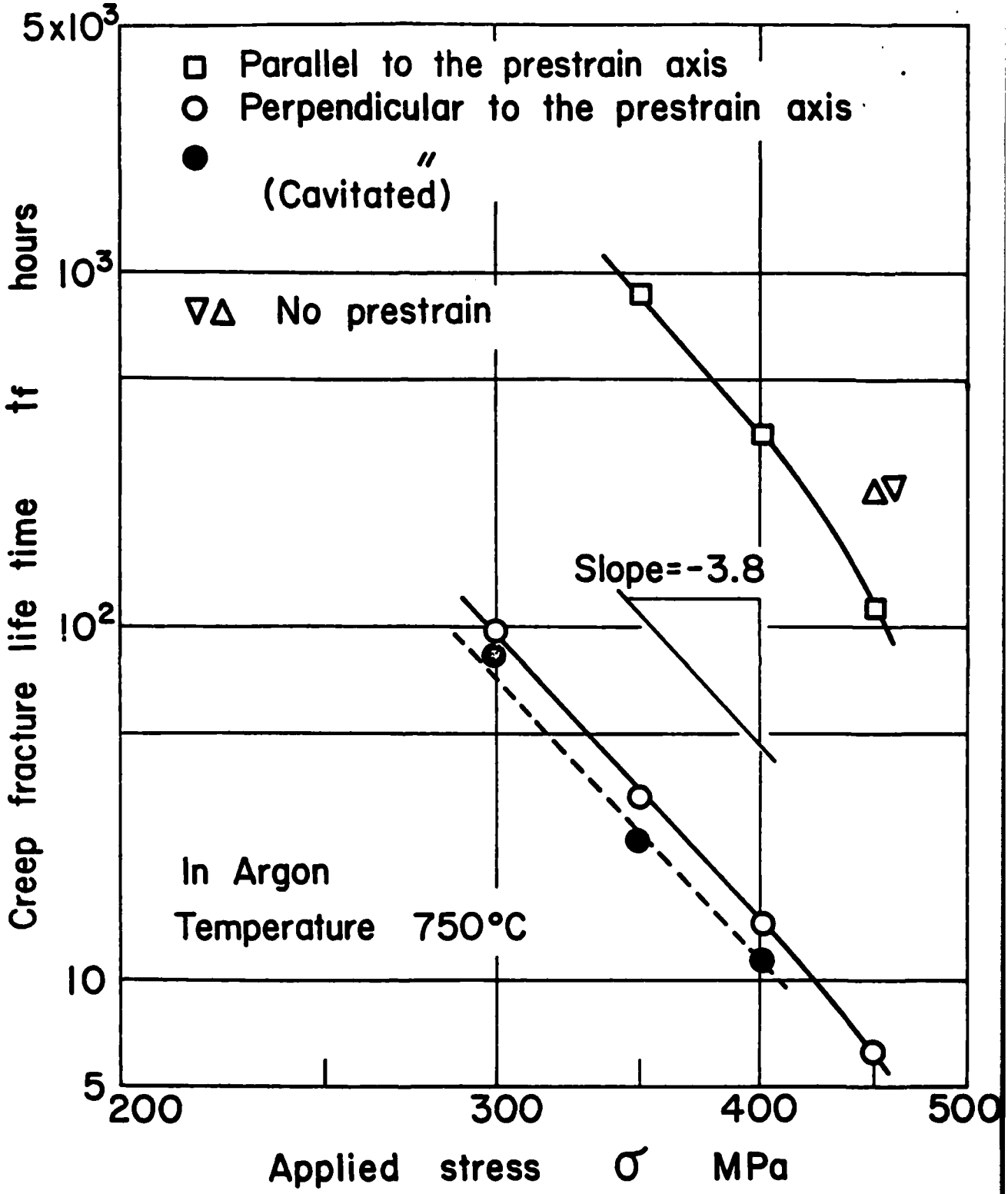

Fig. 18--Creep life, t_f, plotted against applied stress, σ, for astroloy specimens crept at 750°C in purified argon. Specimens had undergone various treatments before creep testing.

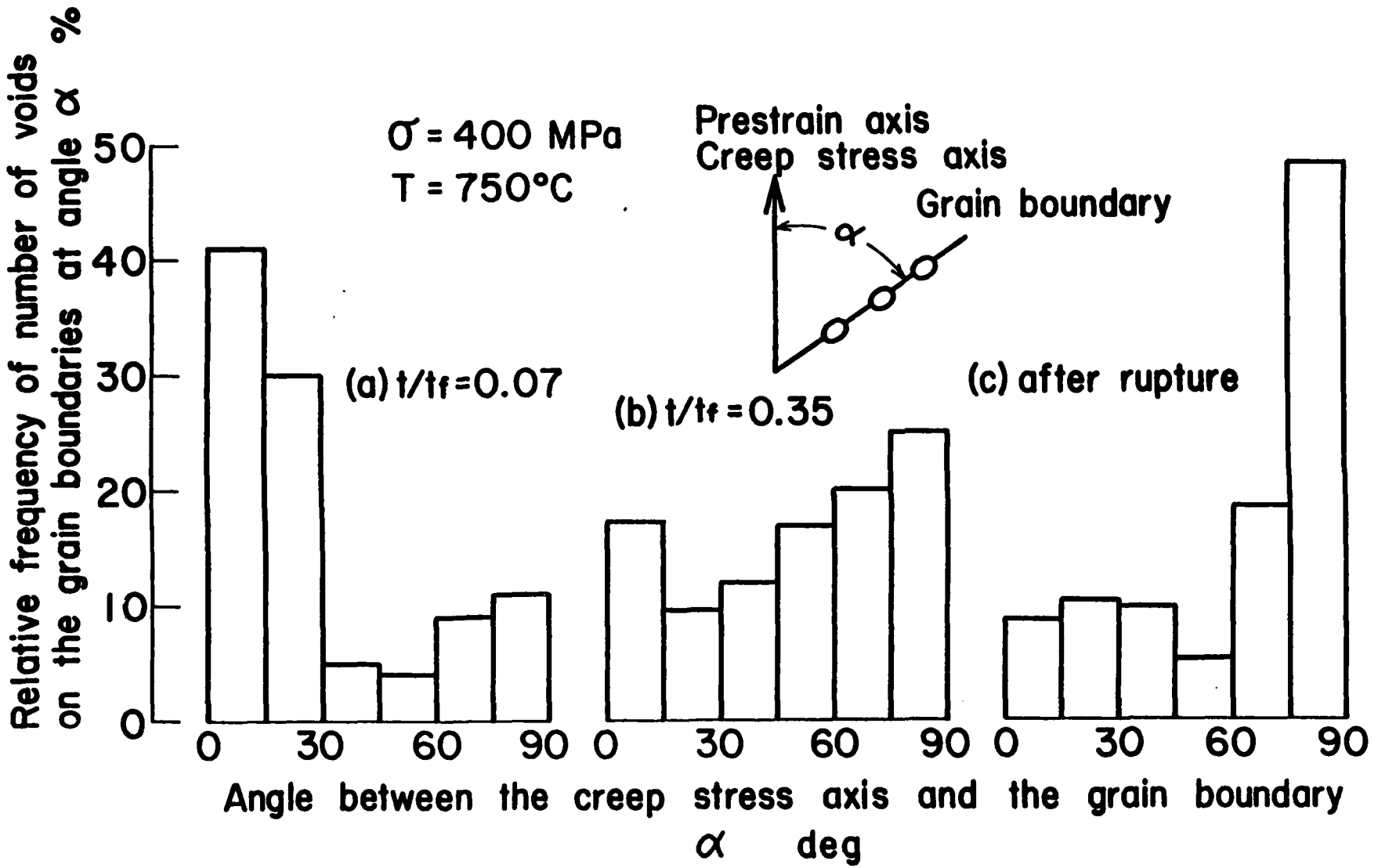

Fig. 19--Relative frequency of cavitation as a function of orientation of the grain boundary trace with respect to the creep stress axis. The astroloy samples had been prestrained 10% parallel to the creep axis, then crept at 750°C under a stress of 400 MPa. From left to right: specimen crept to 7% of life; crept to 35% of life; crept to rupture.

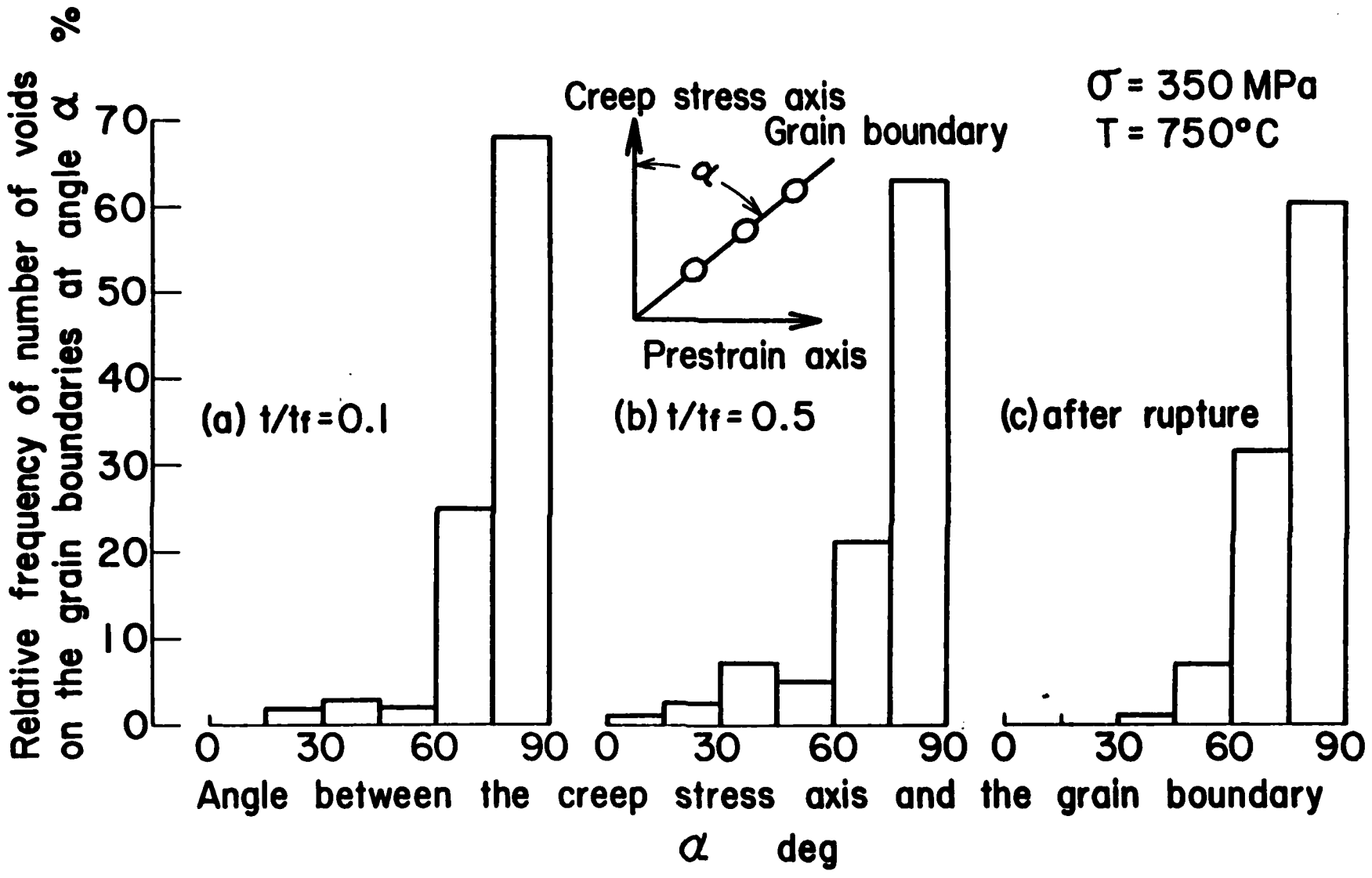

Fig. 20--Relative frequency of cavitation as a function of orientation of the grain boundary trace with respect to the creep stress axis. The astroloy samples had been prestrained 10% in a direction perpendicular to the creep axis, then crept under a stress 350 MPa at 750°C. From left to right: specimen crept to 10% of life; crept to 50% of life; crept to failure.

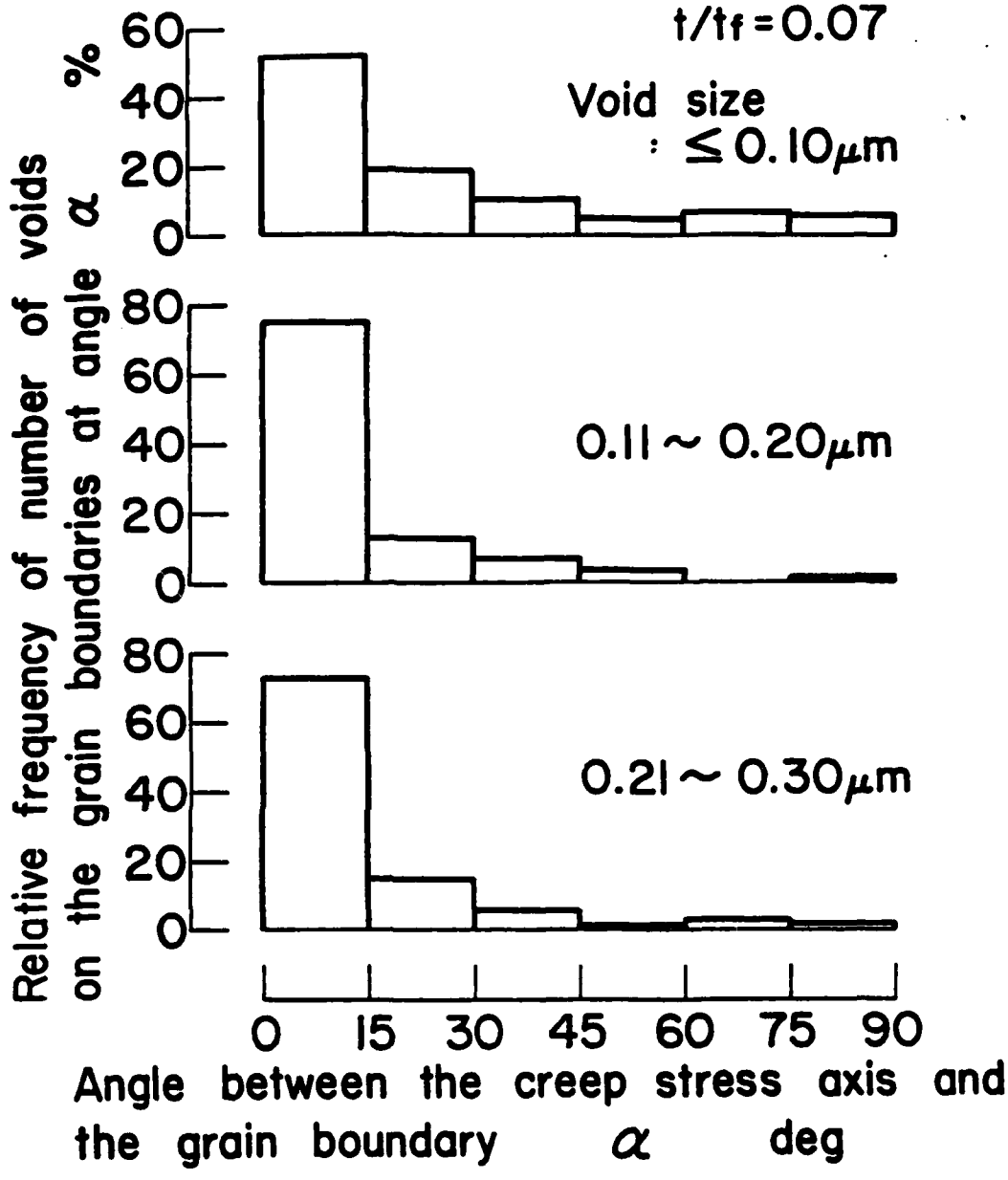

(a)

Fig. 21--Relative frequency of cavitation as a function of orientation of the grain boundary trace with respect to the creep stress axis. Cavities grouped according to size. The astroloy samples had been prestrained 10% parallel to the creep axis, then crept under a stress of 400 MPa at 750°C. (a) Sample crept to 7% of life; (b) crept to 35% of life; (c) crept to rupture.

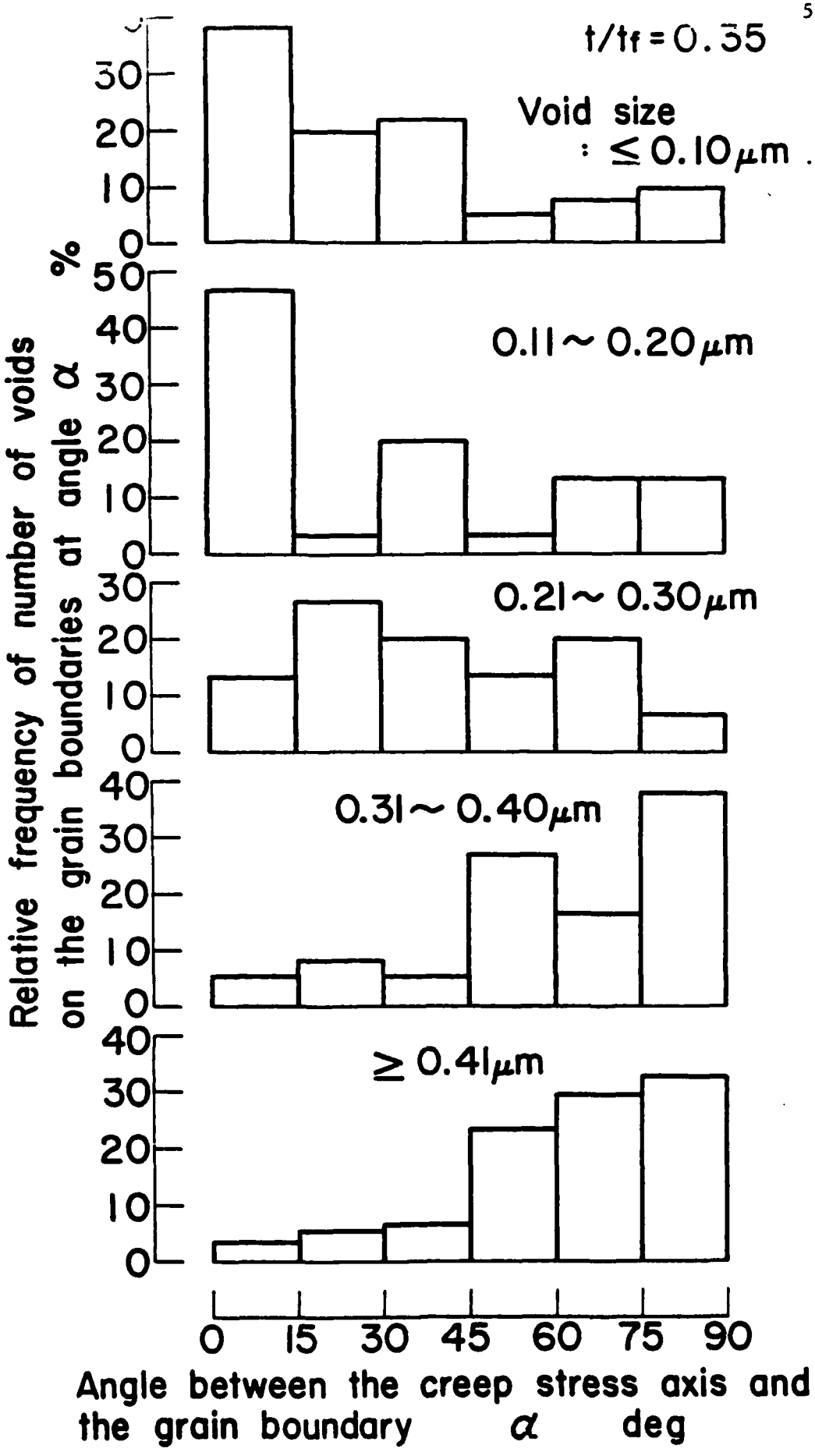
t/tf = 0.35
Void size
: ≤ 0.10μm
0.11 ~ 0.20μm
0.21 ~ 0.30μm
0.31 ~ 0.40μm
≥ 0.41μm
Relative frequency of number of voids on the grain boundaries at angle α %
0 15 30 45 60 75 90
Angle between the creep stress axis and the grain boundary α deg

(b)

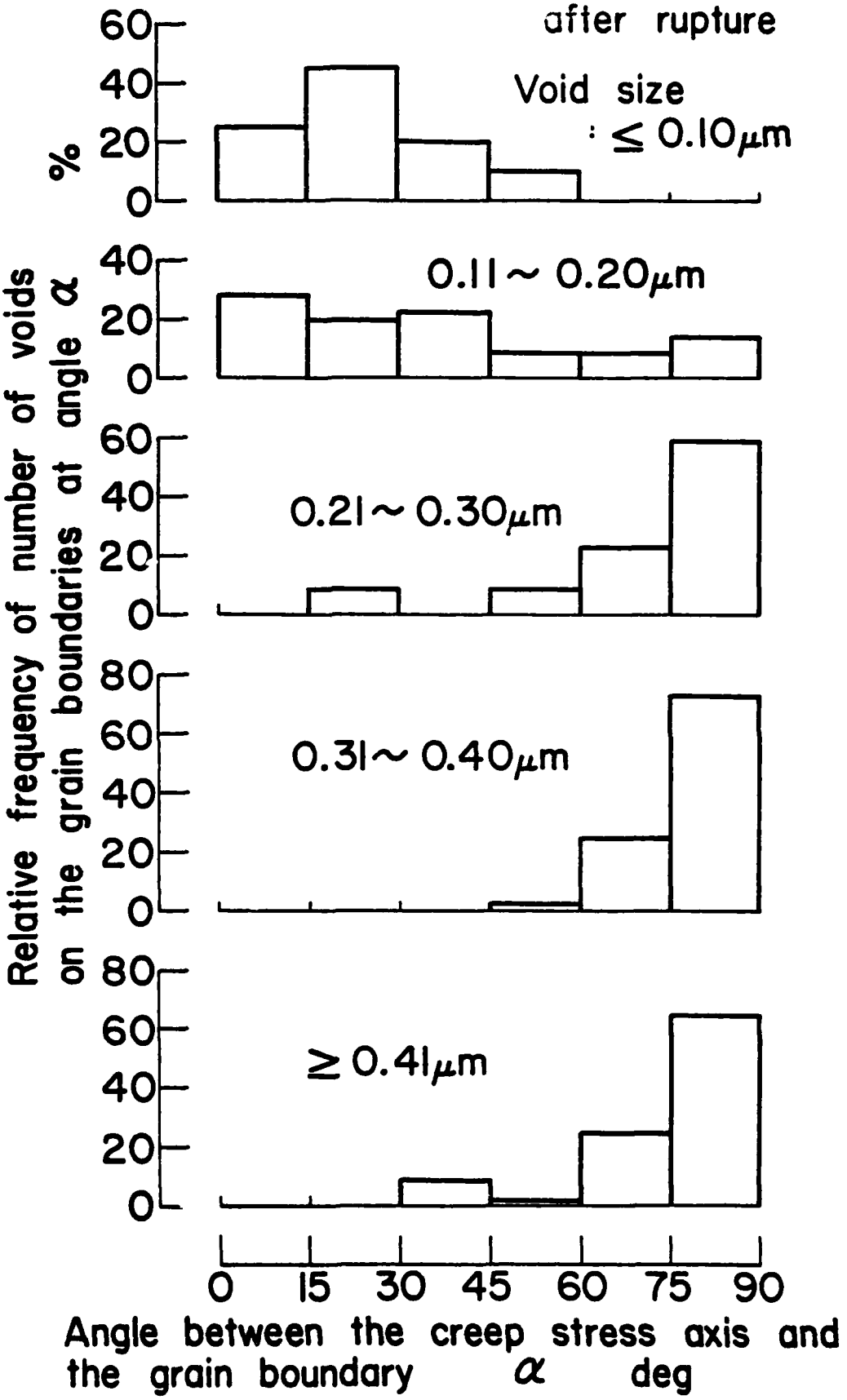
after rupture
Void size
: ≤ 0.10μm
0.11 ~ 0.20μm
0.21 ~ 0.30μm
0.31 ~ 0.40μm
≥ 0.41μm
%
60
40
20
0
80
0 15 30 45 60 75 90
Relative frequency of number of voids on the grain boundaries at angle α
Angle between the creep stress axis and the grain boundary α deg

(c)

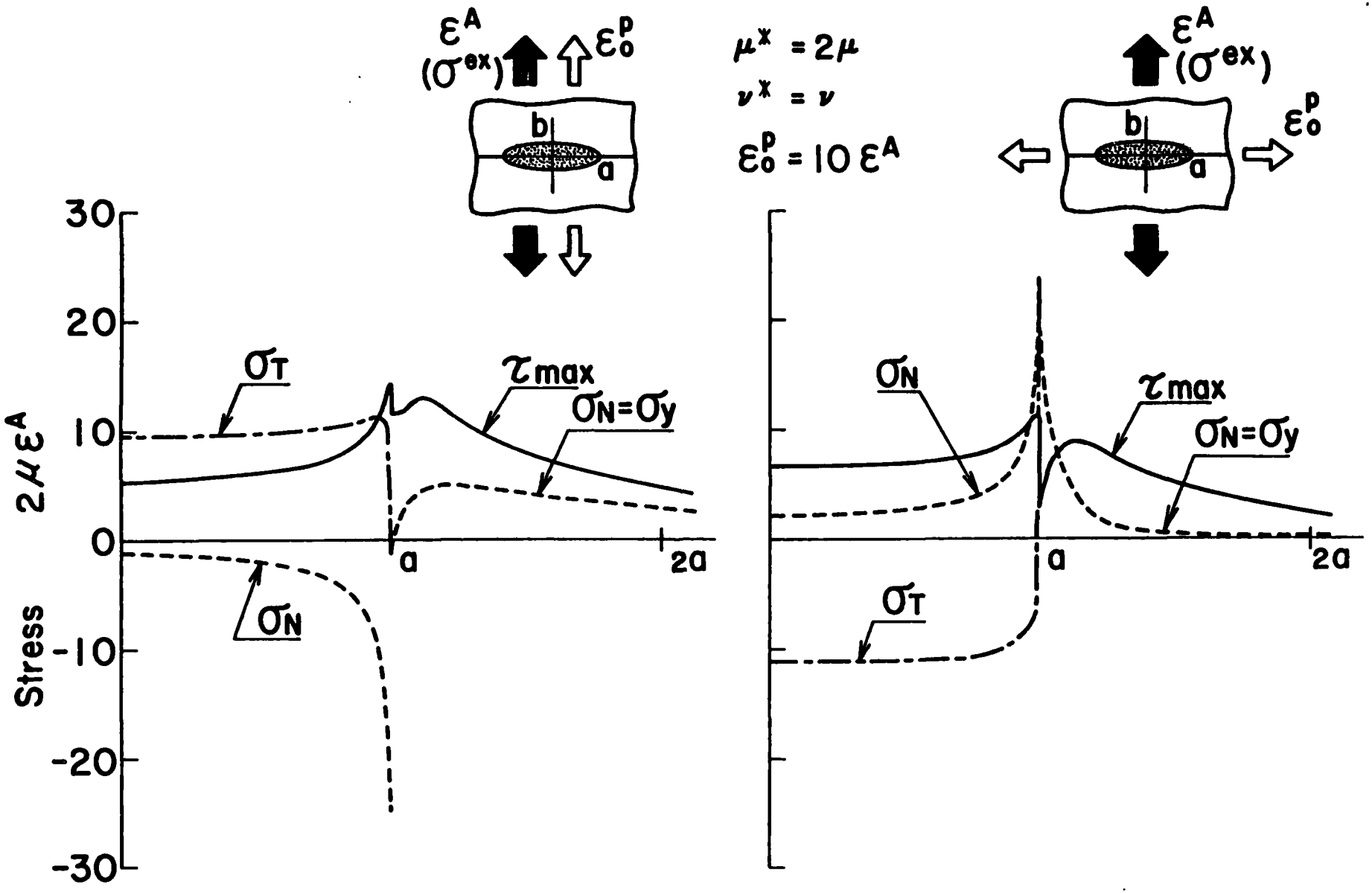

Fig. 22--Normal stress σ_N, tangential stress σ_T, and maximum shear stress τ_{max} which develop at the interface of the inclusion with the matrix after the matrix has suffered a uniform plastic deformation ε_o^p, and the matrix/inclusion ensemble has been pulled by an external stress σ^{ex} to a strain ε^A (far from the inclusion). Orientation of ε_o^p, ε^A, and the long axis of the inclusion as shown in inset drawings. $\varepsilon_o^p = 10\varepsilon^A$.

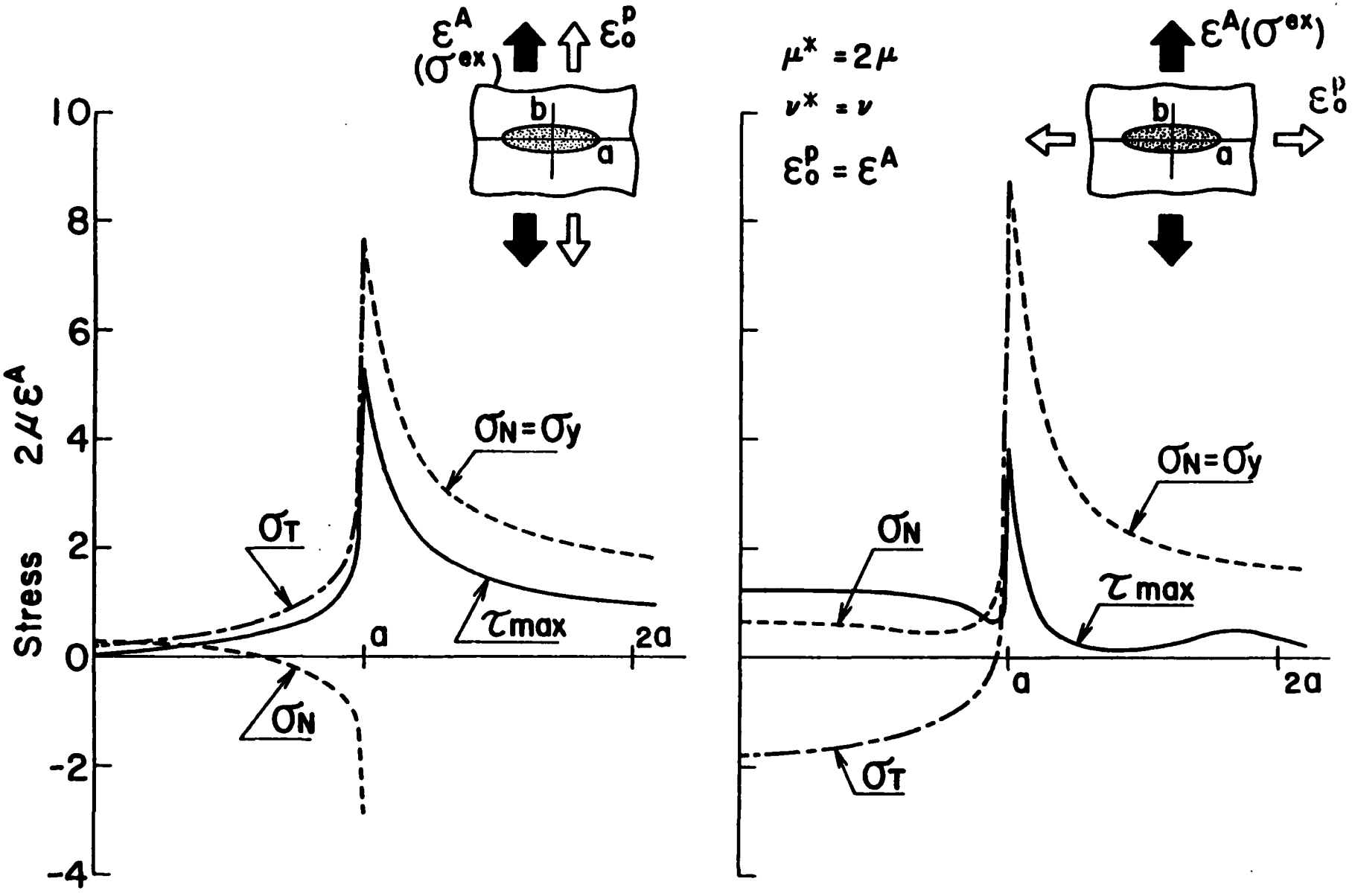

Fig. 23--Same as Figure 22 except that $\varepsilon_o^p = \varepsilon^A$.

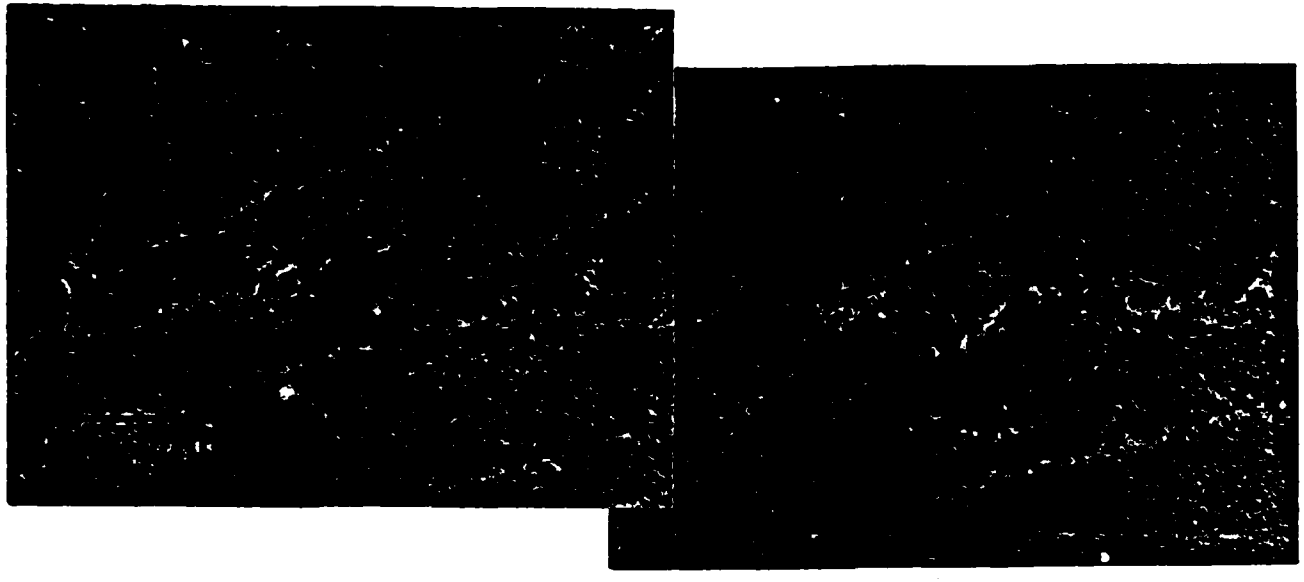

Fig. 24--Shadowed two stage replica of specimen of astroloy crept at 750°C.

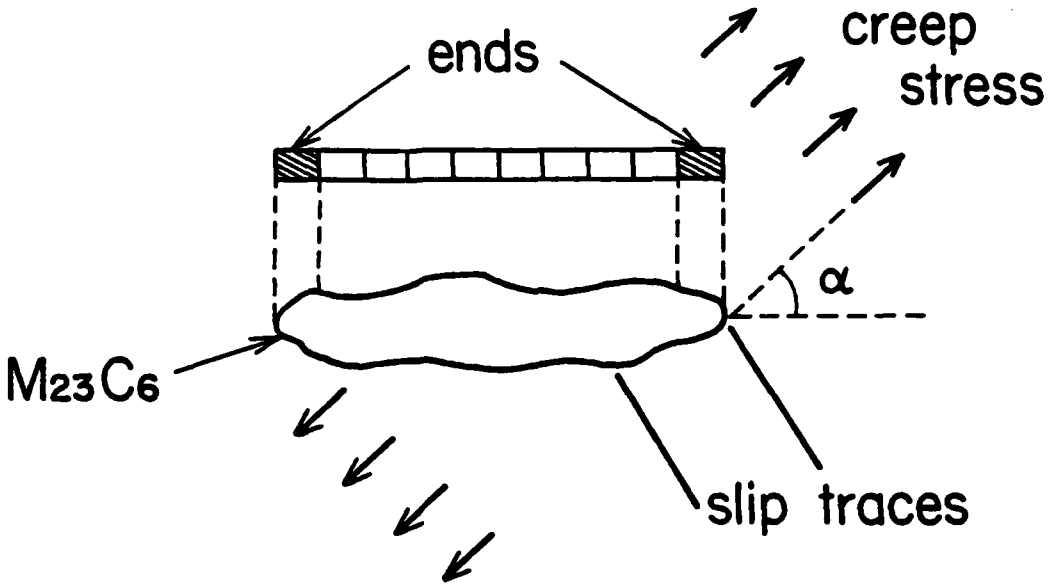

α deg.	% slip traces hitting a carbide end
0°±10°	63 / 79 = 79.7 %
45°±10°	54 / 68 = 79.4 %
90°±10°	118 / 147 = 80.3 %

Fig. 25--Fraction of slip traces hitting the ends of a grain boundary carbide as a function of the angle α between the creep stress axis and the grain boundary trace. The numerator in a fraction is the number of traces observed hitting an end; the denominator is the total number of traces observed.

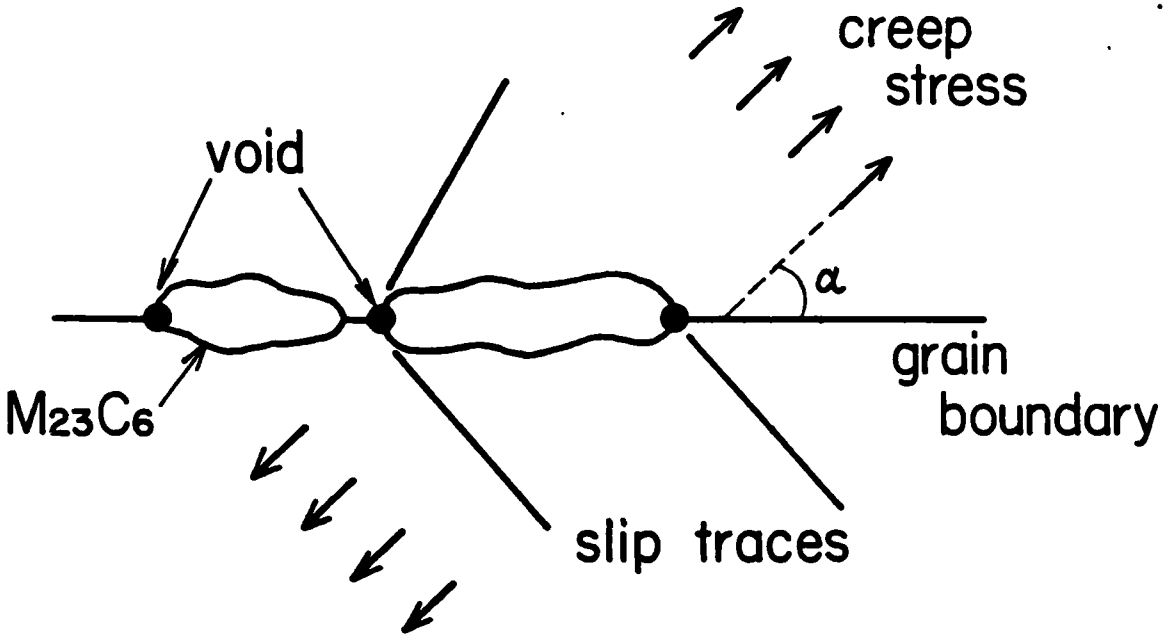

α deg.	void with slip trace(s)	total no. voids	% voids with slip traces
0°-90°	120	172	69.8 %
0°±10°	5	7	71.4 %
45°±10°	31	46	67.4 %
90°±10°	84	119	70.6 %

Fig. 26--Fraction of voids associated with one or two slip traces as a function of the angle α between the creep stress axis and the grain boundary trace.

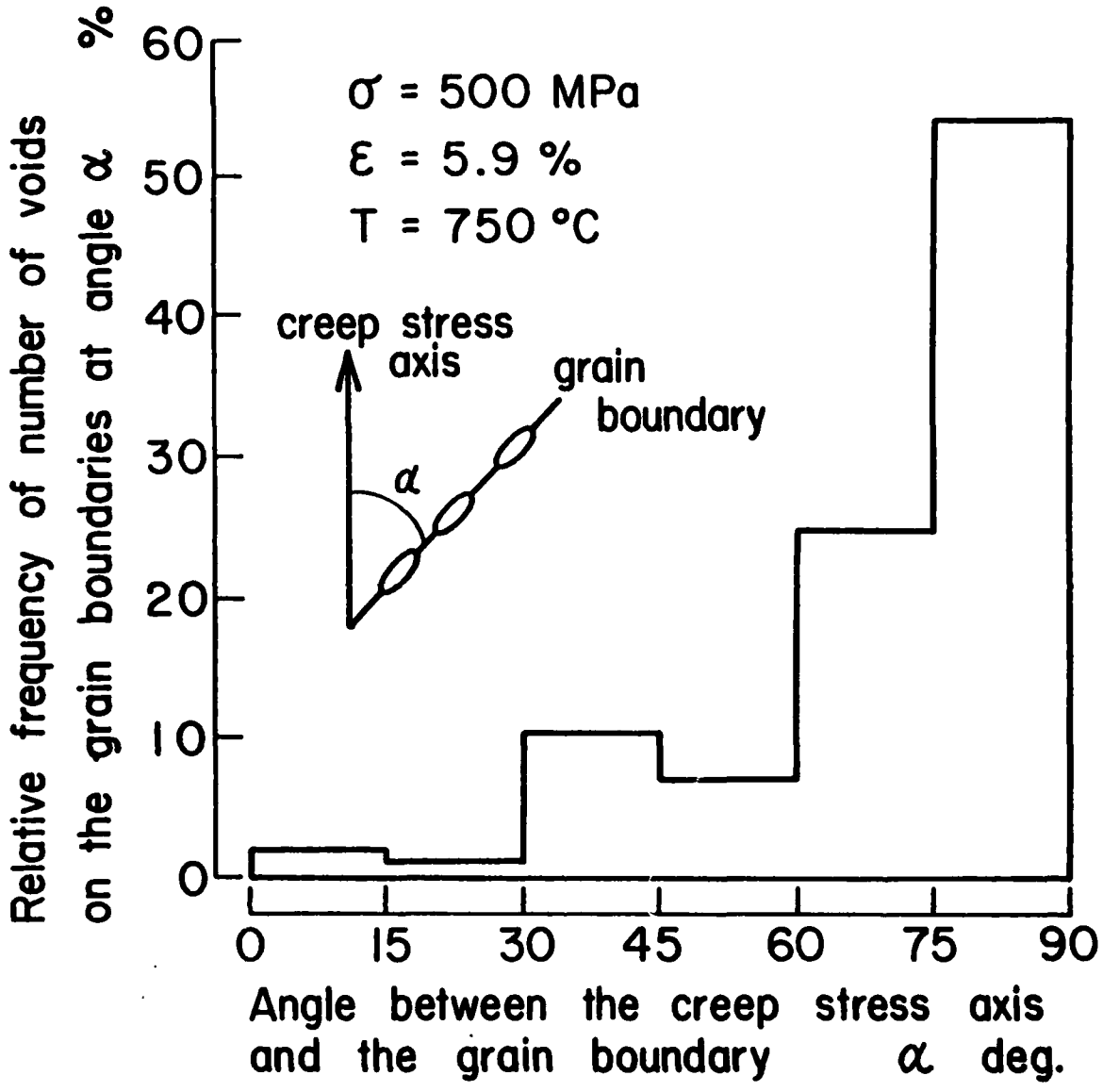

Fig. 27--Relative frequency of cavitation as a function of orientation of the grain boundary with respect to the creep axis. The astroloy specimen was crept at 750°C under a creep stress of 500 MPa to a total creep strain of 5.9%.

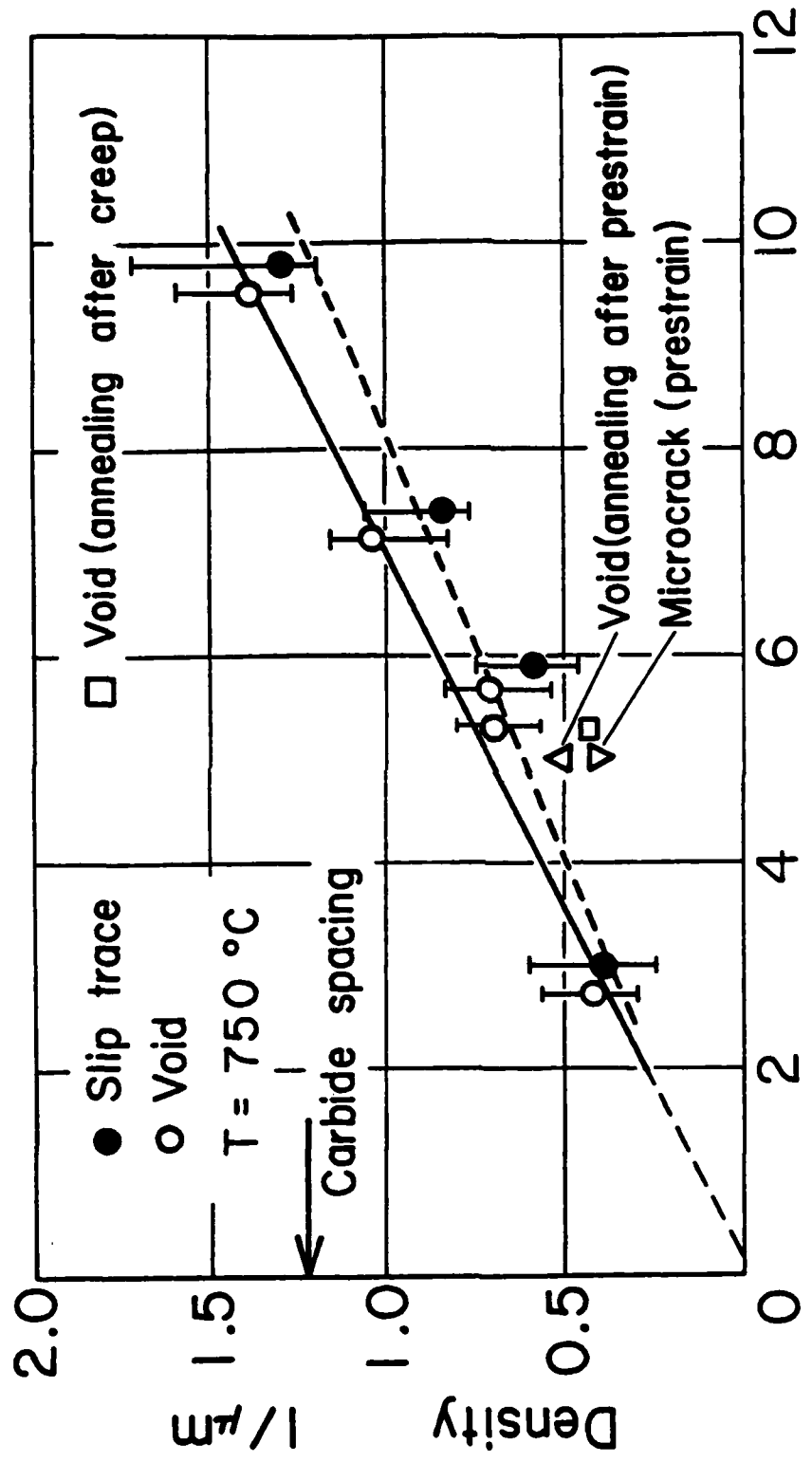

Fig. 28--Void density and slip trace density vs total creep strain in specimens of astroloy crept at 750°C. See text for the creep stress corresponding to each point.

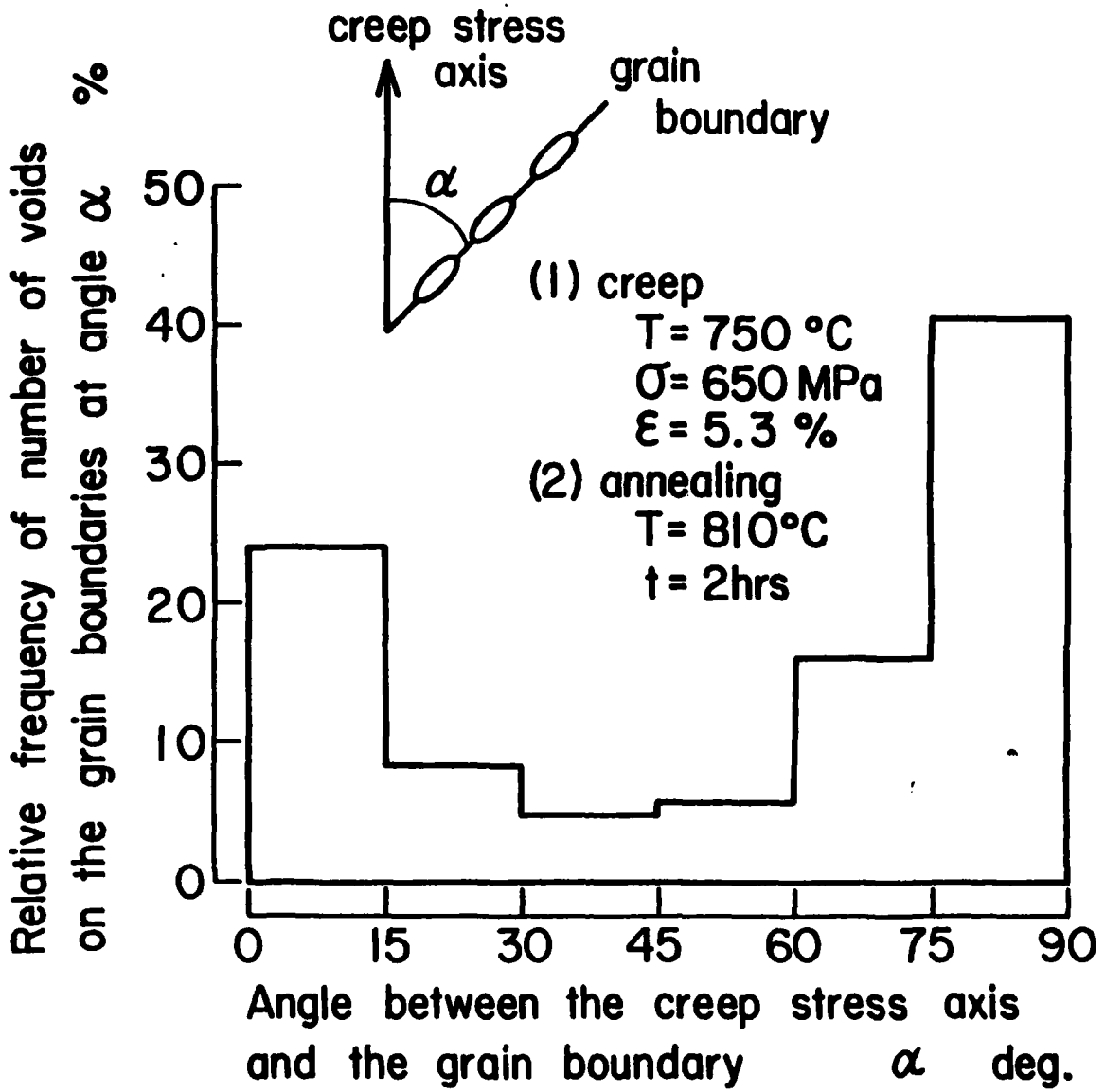

Fig. 29--Relative frequency of cavitation as a function of orientation of the grain boundary with respect to the creep stress axis. The astroloy specimen was crept at 750°C under a creep stress of 650 MPa to a total creep strain of 5.3% and then annealed at 810°C for 2 hours.

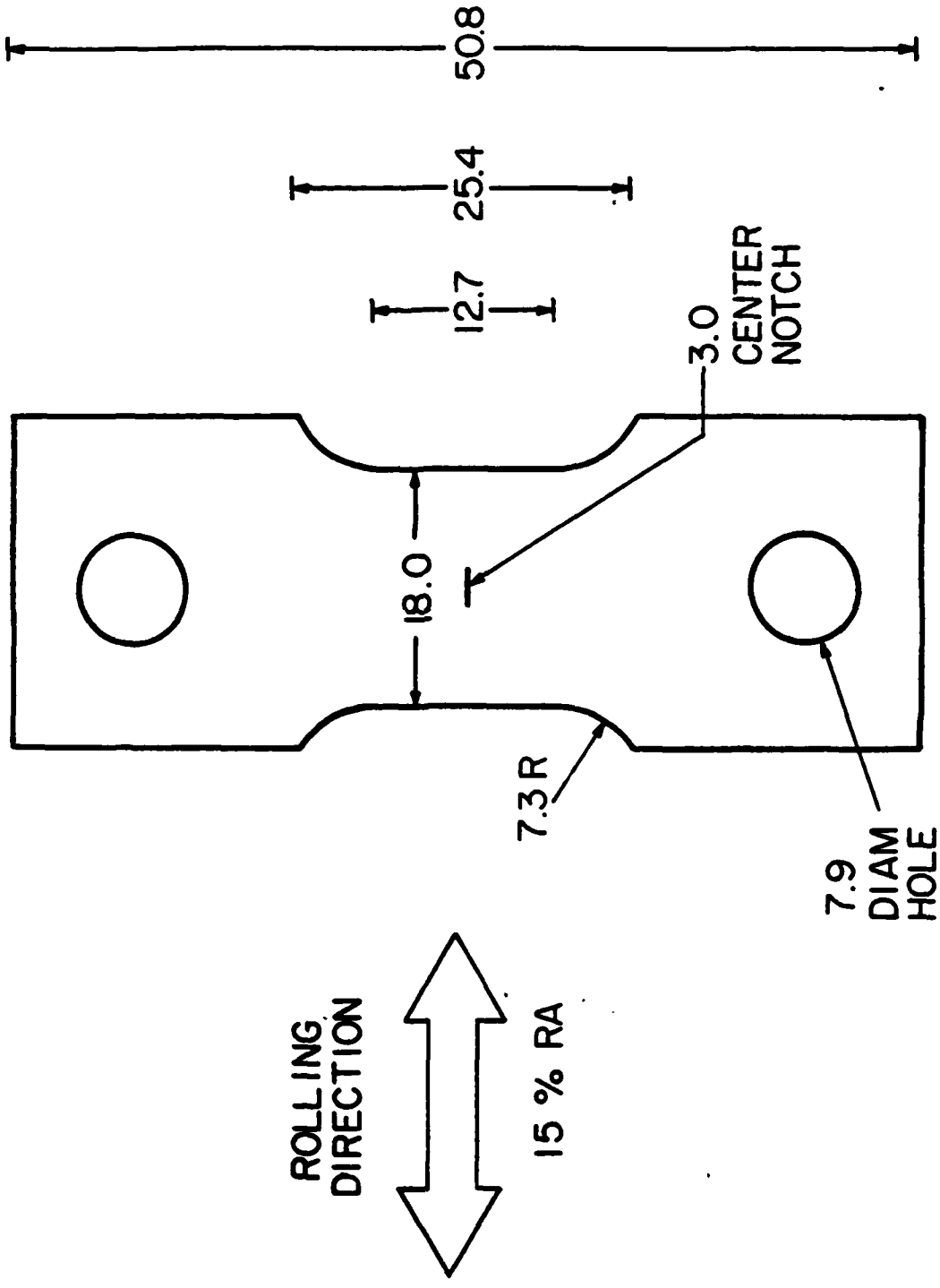

Fig. 30--Center notched fatigue specimen. All dimensions are in mm. The thickness of the specimens is about 3 mm.

Fig. 31--Voids in a sample of H-1 astroloy which has been fatigued 4,000 cycles; K_{max}=32.8 MPa$\sqrt{m}$. The portion of the grain boundary shown in Fig. 31 is ≈ 54μm from the crack tip.

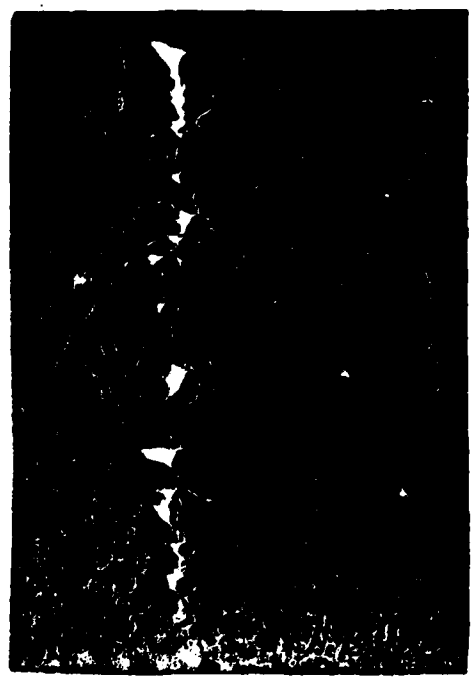

Fig. 32--Coalescing voids in the the sample of Fig. 31.

Fig. 33--Large coalesced voids merging into the crack tip in the sample of Fig. 31.

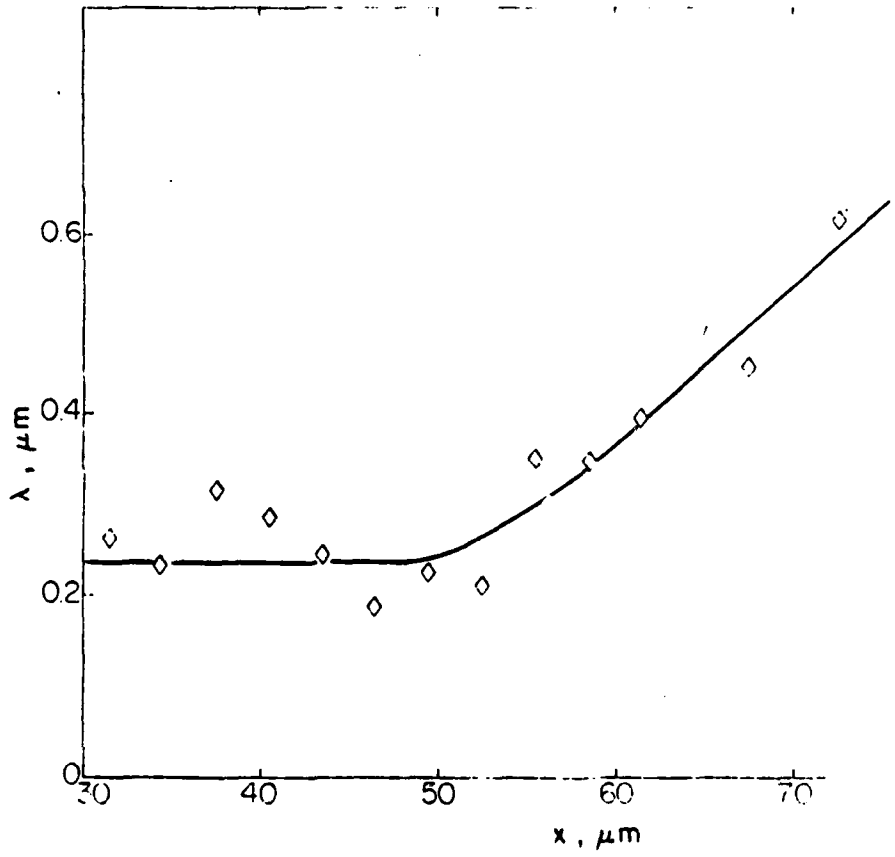

Fig. 34--Spacing λ between individual voids as a function of the distance x from the crack tip. The stress intensity factor at the peak of the loading cycle, K_{max}, is 32.8 MPa$\sqrt{m}$. Precavitated H-1 astroloy fatigued at 6 hz, R = 0, for 15,000 cycles, at 750°C.

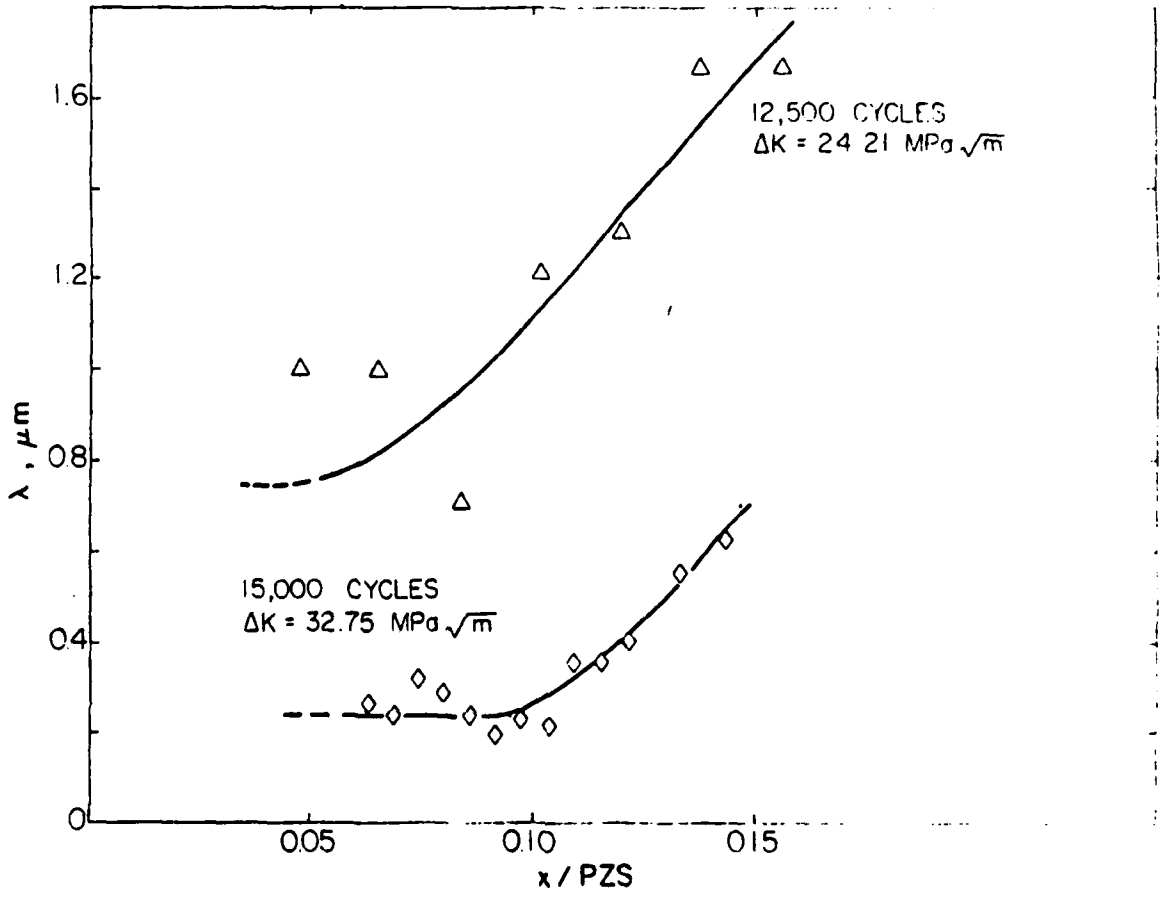

Fig. 35--Spacing λ between individual voids as a function of the distance from the crack tip normalized with respect to the plastic zone size, x/PZS. Upper curve: K_{max} = 24.2 MPa√m, sample fatigued 12,500 cycles. Lower curve: K_{max} = 32.8 MPa√m, sample fatigued 15,000 cycles. Precavitated H-1 astroloy fatigued at 6 hz, R = 0, 750°C.

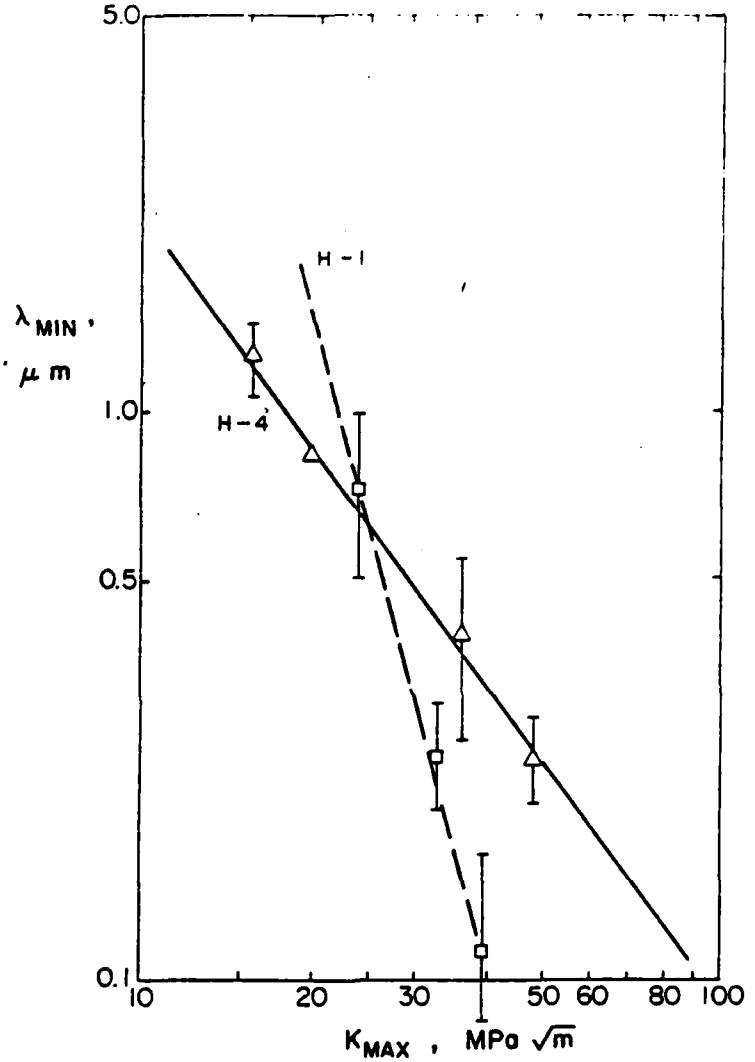

Fig. 36--Minimum spacing of non-coalesced voids, λ_{min}, as a function of K_{max} for H-1 and H-4 astroloy. Precavitated astroloy fatigued at 6 hz, R ≈ 0, 750°C.

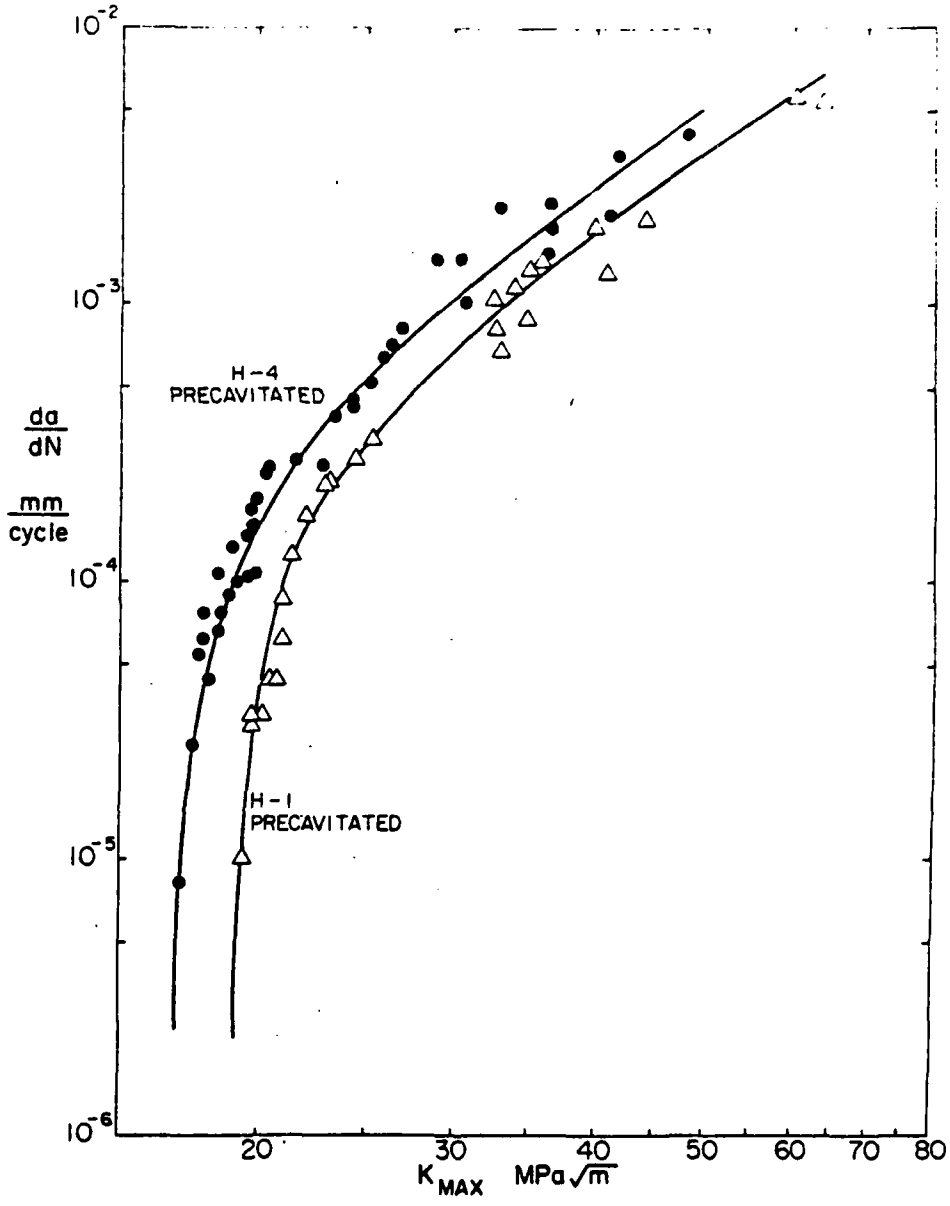

Fig. 37--Crack growth rate per cycle, da/dN, vs K_{max} for precavitated astroloy given the H-1 or H-4 heat treatment. Samples fatigued at 6 hz, R = 0, 750°C.

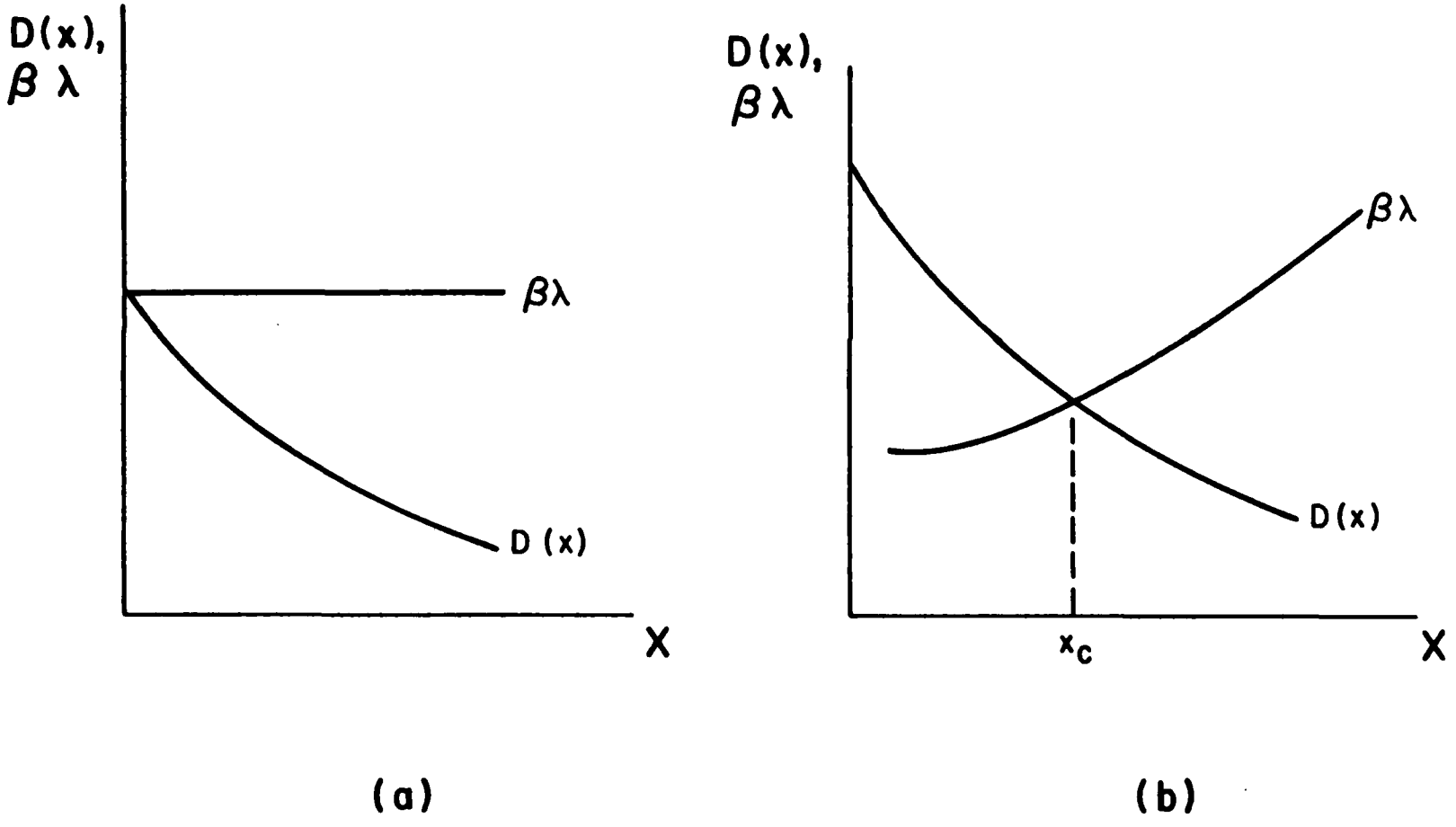

Fig. 38--Displacement across the crack plane, D(x), and βλ as functions of distance x from the crack tip. Here λ is spacing between individual voids and β is a constant. (a) Threshold region of crack propagation. The void spacing has the precavitated value, $\lambda = \lambda_o$. (b) Well beyond threshold.

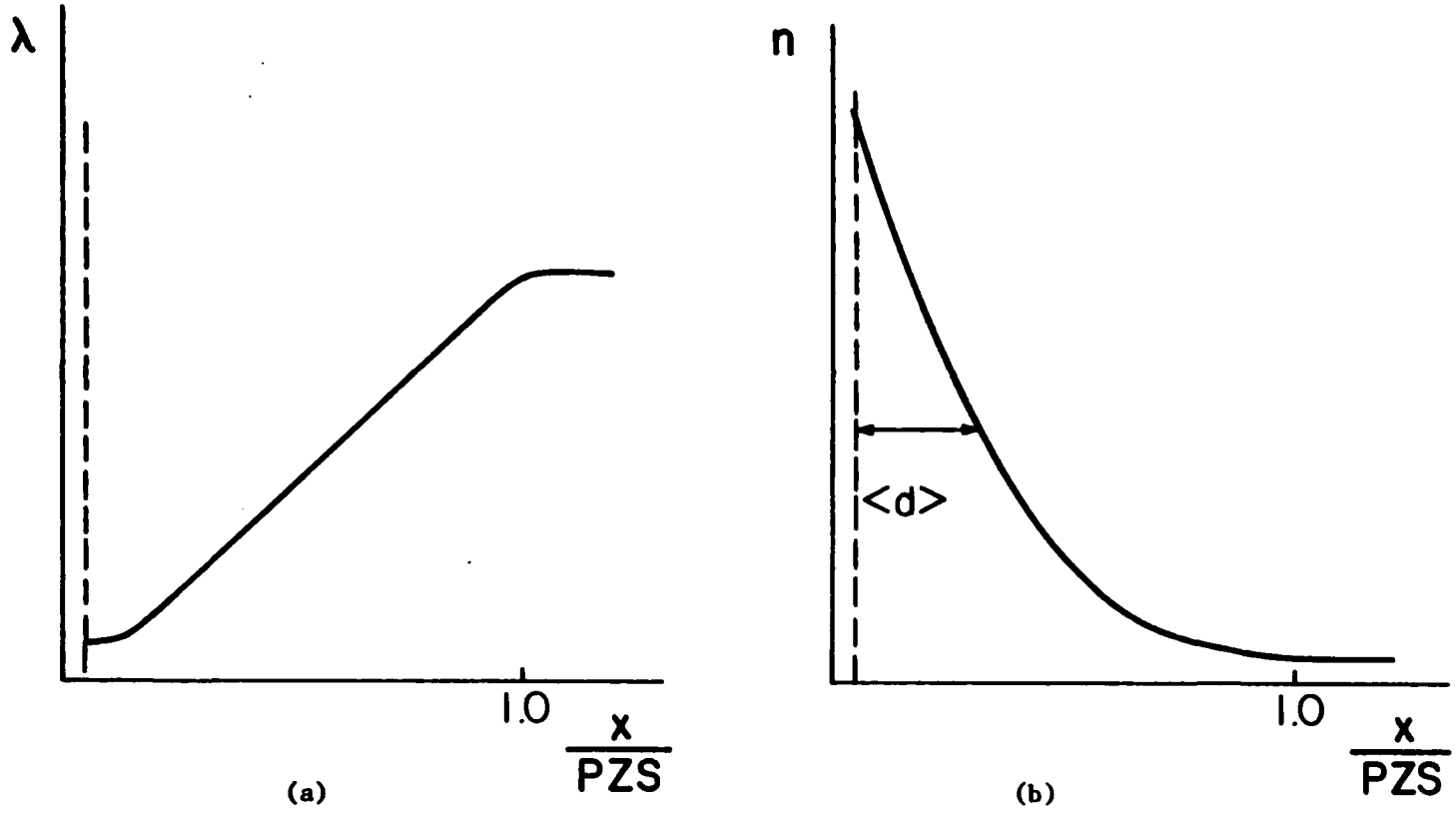

Fig. 39--(a) Schematic plot of the variation of spacing between individual voids, λ, as a function of distance x from the crack tip. The dashed vertical line indicates the value of x where voids begin to coalesce (x_f). (b) Variation of the number of voids per unit area of grain boundary, n, as a function of x. <d> is the average distance a void travels relative to the crack tip from the moment of nucleation until it coalesces with its neighbors.

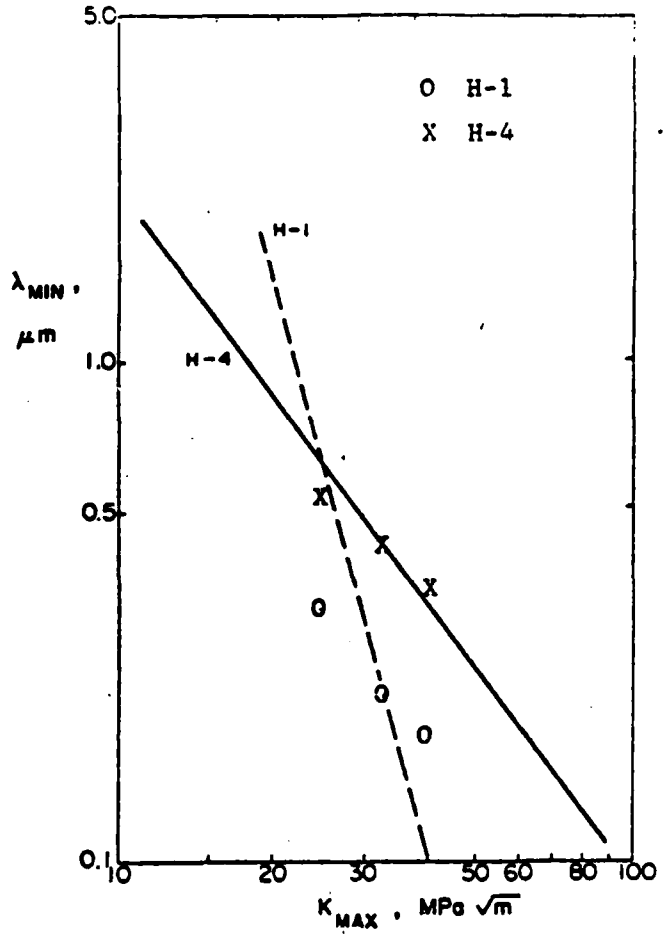

Fig. 40--Solid and dashed curves: experimentally determined curves of λ_{min} vs K_{max} for precavitated H-1 and H-4 astroloy fatigued at 6 hz, T = 750°C, R ≈ 0 (see Fig. 36). Points: values of λ_{min} which, when used in Eqns. 3 to 6, lead to calculated values of da/dN equal to the measured rates of crack growth per cycle.

PERSONNEL

Principal Investigator

Julia Weertman

Secretaries

Mary Pahl (partial support)

Beth Goldberg (partial support)

Graduate Research Assistant

Brad Kirkwood

Postdoctoral Fellows

M. Uemura

T. Saegusa

M. Kikuchi

K. Shiozawa

PUBLICATIONS AND DISSERTATION

"Grain Boundary Void Nucleation in Astroloy Produced by Room Temperature Deformation and Anneal," T. Saegusa, M. Uemura, and J. R. Weertman, Metallurgical Transactions 11A, 1453 (1980).

"Mechanism for Nucleation of Grain Boundary Voids in a Nickel Base Superalloy," M. Kikuchi and J. R. Weertman, Scripta Metallurgica 14, 797 (1980).

"Void Nucleation in Astroloy: Theory and Experiments," M. Kikuchi, K. Shiozawa, and J. R. Weertman, Acta Metallurgica 29, 1747 (1981).

"Observation of Grain Boundary Microcracking in a Nickel Base Superalloy after Room Temperature Deformation," K. Shiozawa and J. R. Weertman, Scripta Metallurgica 15, 1241 (1981).

"The Nucleation of Grain Boundary Voids in Astroloy during High Temperature Creep," K. Shiozawa and J. R. Weertman, Scripta Metallurgica 16, 735 (1982).

"Studies of Nucleation Mechanisms and the Role of Residual Stresses in the Grain Boundary Cavitation of a Superalloy", to be published.

"Deformation-Induced Strain Localization and Residual Stresses around Hard Particles," K. Shiozawa and J. R. Weertman, Proceedings of Workshop on Plasticity of Metals at Finite Strain, June 29-July 1, 1981, Stanford University, in press.

"Nucleation of Grain Boundary Voids in the Vicinity of an Intergranular Fatigue Crack," B. Kirkwood and J. R. Weertman, Scripta Metallurgica 16, 627 (1982).

"Cavity Nucleation during Fatigue Crack Growth Caused by Linkage of Grain Boundary Cavities," B. Kirkwood and J. R. Weertman, Micro and Macro Mechanics of Crack Growth, edited by K. Sadananda, D. J. Michel and B. B. Rath, TMS-AIME, New York p. 199, 1982.

Ph.D. Dissertation, Brad Kirkwood, June 1982, "High Temperature Fatigue Crack Propagation in a Nickel Base Superalloy and Investigation of the Intergranular Fracture Process".

ORAL PRESENTATIONS

"Grain Boundary Void Nucleation in Astroloy Produced by Room Temperature Deformation and Anneal", (presented by T. Saegusa), AIME meeting, St. Louis, MO, 16 October 1978.

"Grain Boundary Void Nucleation Produced by Room Temperature Deformation and Anneal", Society of Engineering Science Annual Meeting, Evanston, IL, 5 September 1979 (invited).

"Slip Band-Void Relationship in Deformed and Annealed Astroloy", (presented by M. Kikuchi), AIME meeting, Las Vegas, NV, 25 February 1980.

"Effect of Cavitation on High Temperature Fatigue Crack Growth", (presented by B. Kirkwood), AIME meeting, Pittsburgh, PA, 9 October 1980.

"Fracture of Ni-Base Superalloy", (presented by M. Uemura), Japan Institute of Metals, 10 October 1980.

"Nucleation and Growth of Voids during the High Temperature Creep of Astroloy", (presented by K. Shiozawa), AIME Annual Meeting, Chicago, IL, 23 February 1981.

"Grain Boundary Cavitation in Metals and Alloys", Metal Science Club of New York, New York, NY, 2 April 1981 (invited).

"Deformation-Induced Strain Localization and Residual Stresses around Hard Particles", Workshop on Plasticity of Metals at Finite Strain, Stanford University, Palo Alto, CA, 1 July 1981 (invited).

"Cavity Nucleation during Fatigue Crack Growth Caused by Linkage of Grain Boundary Cavities", AIME/TMS Fall Meeting, Louisville, KY, 15 October 1981.

"Strain Induced Microcracking at Inclusions: Theory and Experiments", Colloquia in Metallurgy, Exxon Research and Engineering Co., Corporate Research Science Lab, Linden, NJ, 6 November 1981 (invited).

"Fatigue Crack Propagation by Grain Boundary Void Coalescence", University of Wisconsin/Milwaukee, Milwaukee, WI, 10 December 1981 (invited).

"Fatigue Crack Growth by Linkage of Grain Boundary Cavities", Department of Ceramics, University of Illinois, Urbana, IL, 29 January 1982 (invited).

"Cavity Nucleation during Fatigue Crack Growth", Oak Ridge National Laboratory, Oak Ridge, TN, 8 April 1982 (invited).

"Void Nucleation and Growth in Metals and Alloys", Alcoa Technical Center, Pittsburgh, PA, 4 June 1982 (invited).